Article

Not peer-reviewed version

Microparticles Released by Dengue Virus-Infected Monocytes Mediate Endothelial Viral Infection and Vasculopathy

Janet García-Pillado , Pedro Pablo Martínez-Rojas , Elizabeth Quiroz-Garcia , Carlos Cabello-Gutiérrez , Marcela Lizano , Luis Padilla-Noriega , Lourdes Teresa Agredano-Moreno , Luis Felipe Jiménez-García , Blanca H. Ruiz-Ordaz *

Posted Date: 30 April 2026

doi: 10.20944/preprints202604.2219.v1

Keywords: dengue; dengue virus; severe dengue; monocytes; endothelial vascular cells; extracellular vesicles; microparticles; microparticles mediating viral dissemination; procoagulant and proinflammatory phenotype; vasculopathy

 doi:10.20944/preprints202604.2219.v1

Article

Microparticles Released by Dengue Virus-Infected Monocytes Mediate Endothelial Viral Infection and Vasculopathy

Janet García-Pillado [1], Pedro Pablo Martínez-Rojas [1], Elizabeth Quiroz-Garcia [1], Carlos Cabello-Gutiérrez [2], Marcela Lizano [3], Luis Padilla-Noriega [4], Lourdes Teresa Agredano-Moreno [5], Luis Felipe Jiménez-García [5] and Blanca H. Ruiz-Ordaz [1,*]

[1] Departamento de Biología Molecular y Biotecnología, Instituto de Investigaciones Biomédicas, Universidad Nacional Autónoma de México, Ciudad de México 04510, México

[2] Departamento de Investigación en Virología y Micología, Instituto Nacional de Enfermedades Respiratorias "Ismael Cosío Villegas", Ciudad de México 14080, México

[3] Departamento de Medicina Genómica y Toxicología Ambiental, Instituto de Investigaciones Biomédicas, Universidad Nacional Autónoma de México, Ciudad de México 04510, México

[4] Departamento de Microbiología y Parasitología, Facultad de Medicina, Universidad Nacional Autónoma de México, Ciudad de México 04510, México

[5] Departamento de Biología Celular, Facultad de Ciencias, Universidad Nacional Autónoma de México, Coyoacán, Ciudad de México CP 04510, México

* Correspondence: bhro@unam.mx; Tel.: +52-155-56228931

Abstract

Dengue is the most prevalent arthropod-borne viral disease, caused by infection with dengue virus (DENV). Severe dengue is characterized by significant vasculopathy involving a proinflammatory and procoagulant state associated with increased vascular permeability. However, the host–virus interactions driving this process remain incompletely elucidate. Monocytes are primary target cells during DENV infection and actively release extracellular vesicles, like microparticles (MPs), mediating intercellular communication contributing to dengue pathogenesis. Here, we evaluated whether MPs released by DENV-infected monocytes represent a previously underappreciated mechanism contributing to dengue-associated vascular dysfunction. The vascular endothelium plays a determining role in the response to injury because it functions as a regulatory interface during hemostasis (coagulation–fibrinolysis–inflammation) and by preserving endothelial barrier. We found that these vesicles transport viral components capable of mediating DENV endothelial vascular cells (EVC) infection, while simultaneously exhibiting a procoagulant profile promoting thrombin generation and cell activation. DENV-infected Mø MPs interaction induces a shift toward a procoagulant, proinflammatory, and proadherent phenotype, characterized by increased expression of PAR-1, TF, ICAM-1, and VCAM-1, reflecting the establishment of a sustained EVC activation that compromises vascular barrier integrity, leading to increased permeability, a hallmark of DENV-associated vasculopathy and a central event in the progression to severe dengue.

Keywords: dengue; dengue virus; severe dengue; monocytes; endothelial vascular cells; extracellular vesicles; microparticles; microparticles mediating viral dissemination; procoagulant and proinflammatory phenotype; vasculopathy

1. Introduction

Dengue, also referred to as dengue fever (DF), is an acute febrile and systemic mosquito-borne viral disease caused by infection with any of the four antigenically distinct dengue virus (DENV) serotypes. DENV is a positive-sense, single-stranded RNA virus that belongs to the genus

 doi:10.20944/preprints202604.2219.v1

Orthoflavivirus within the *Flaviviridae* family [1,2]. According to the World Health Organization (WHO), approximately 50% of the global population is currently at risk of DENV infection, with an estimated 100–400 million infections occurring annually. Dengue is considered endemic in more than 130 countries worldwide [1].

Viral transmission occurs primarily through the bite of infected *Aedes* spp. mosquitoes, and infection can result in a broad spectrum of clinical manifestations, ranging from asymptomatic or mild illness to severe dengue (SD), previously known as dengue shock syndrome (DSS) and dengue hemorrhagic fever (DHF). SD may involve plasma leakage, hemorrhage, organ impairment, and potentially fatal outcomes [3,4].

The pathogenesis of SD is characterized by high levels of viremia associated with inefficient viral clearance, together with marked activation of DENV target cells such as monocytes [5–7], macrophages, dendritic cells [8,9], and platelets [10,11], leading to increased production of proinflammatory cytokines. These events contribute to hemostatic disturbances, including thrombocytopenia, dysregulation of the coagulation–inflammation systems, and vascular damage [12]. Consequently, interactions between DENV-infected cells and vascular endothelial cells disrupt the endothelial basal state—characterized by anticoagulant and anti-inflammatory functions and preserved barrier integrity—promoting a vasculopathy defined by a procoagulant and proinflammatory phenotype with increased vascular permeability and plasma extravasation [13].

Monocytes (Mø) function as key regulators of the host response by contributing to viremia control while simultaneously acting as central drivers of immunopathology. Beyond their antiviral role, activated and DENV-infected monocytes can amplify inflammatory signaling, facilitate antibody-dependent enhancement (ADE) of infection, and promote endothelial dysfunction, processes described in SD [5,6]. Accordingly, monocytes respond to DENV infection by becoming activated and undergoing differentiation [7,14,15], leading to the expression of multiple bioactive products, including inflammatory mediators [16], coagulation-associated proteins such as Tissue Factor [17,18], and the release of extracellular vesicles (EVs) [19].

Extracellular vesicles (EVs) are cell-derived, lipid bilayer–enclosed particles released into the extracellular milieu that lack autonomous replicative capacity [20]. Functionally, EVs are increasingly recognized as active mediators of intercellular communication, capable of transferring bioactive cargo that modulates inflammatory, immune, and vascular responses, thereby contributing to both homeostatic regulation and disease pathogenesis [21]. Based on their biogenesis, EVs are broadly classified into small EVs (sEVs), commonly referred to as exosomes, which originate from the endosomal pathway, and large EVs (lEVs), also termed ectosomes, microparticles, or microvesicles, which are generated by direct outward budding from the plasma membrane [22,23].

Microparticles (MPs) are increasingly recognized as key players in the pathogenesis of vascular diseases associated with chronic inflammation, endothelial damage, and thrombosis [24,25]. MPs are released by multiple cell types, with platelet-derived MPs representing the most abundant population in circulation and being primarily associated with procoagulant activity. During DENV infection, platelet activation drives the release of MPs that contribute to inflammation and endothelial dysfunction, both tightly associated with disease severity [26]. Hottz et al. (2013) demonstrated that platelet-derived MPs generated, via mitochondrial oxidative signaling and inflammasome activation, the increase of endothelial permeability and correlate with plasma leakage and elevated hematocrit levels in severe dengue, supporting their value as biomarkers of disease progression [27]. Other reports have shown that MPs released from erythrocytes and platelets frequently expose phosphatidylserine (PS) and viral antigens: elevated erythrocyte MPs correlate with disease severity and complement activation, while reduced platelet MPs are associated with bleeding manifestations linked to thrombocytopenia [28,29].

However, the functional contribution of monocyte-derived MPs released during DENV infection to endothelial injury and barrier dysfunction remains poorly understood. Likewise, we previously reported that during *in vitro* ZIKV infection, activated intermediate Mø release exosomes that carry viral components as part of their cargo. The naïve-cell–exosomes interaction promotes viral

 doi:10.20944/preprints202604.2219.v1

transmission, infection, and cell differentiation/activation. Hence, exosomes derived from ZIKV-infected Mø are an efficient alternative transmission route that may contribute to disease progression [30].

Based on the evidence supporting a role for MPs in dengue-associated vascular dysfunction, we hypothesized that MPs released by DENV-infected monocytes contribute both to endothelial injury and barrier disruption and the possible viral elements (RNA) which promotes viral dissemination. Therefore, the aim of this study was to determine the role of monocyte-derived MPs in mediating DENV endothelial infection and activation. To address this, we employed *in vitro* models of monocyte infection and endothelial cell stimulation to evaluate the impact of monocyte-derived MPs on vascular damage and loss of barrier permeability (vasculopathy) associated with the pathogenesis of SD.

2. Results

2.1. Dengue Virus (DENV) Infection Induces Procoagulant and Proinflammatory Phenotype in Monocytes

First, we performed an *in vitro* infection of 1.0 × 10^6 monocytes (Mø) with DENV-2 under previously established optimal conditions (MOI of 1, 72 h incubation at 37 °C and 5% of CO_2) and evaluated the presence of the viral envelope (E) and nonstructural 1 (NS1) proteins at cell membrane surface and found that 61% of DENV-infected Mø (DENV-2 Mø) were E+ ($p < 0.0001$) (Figure 1A–B) and 43% were NS1+ ($p < 0.0001$) (Figure 1C–D). These viral components were not detected in uninfected cells (Control Mø).

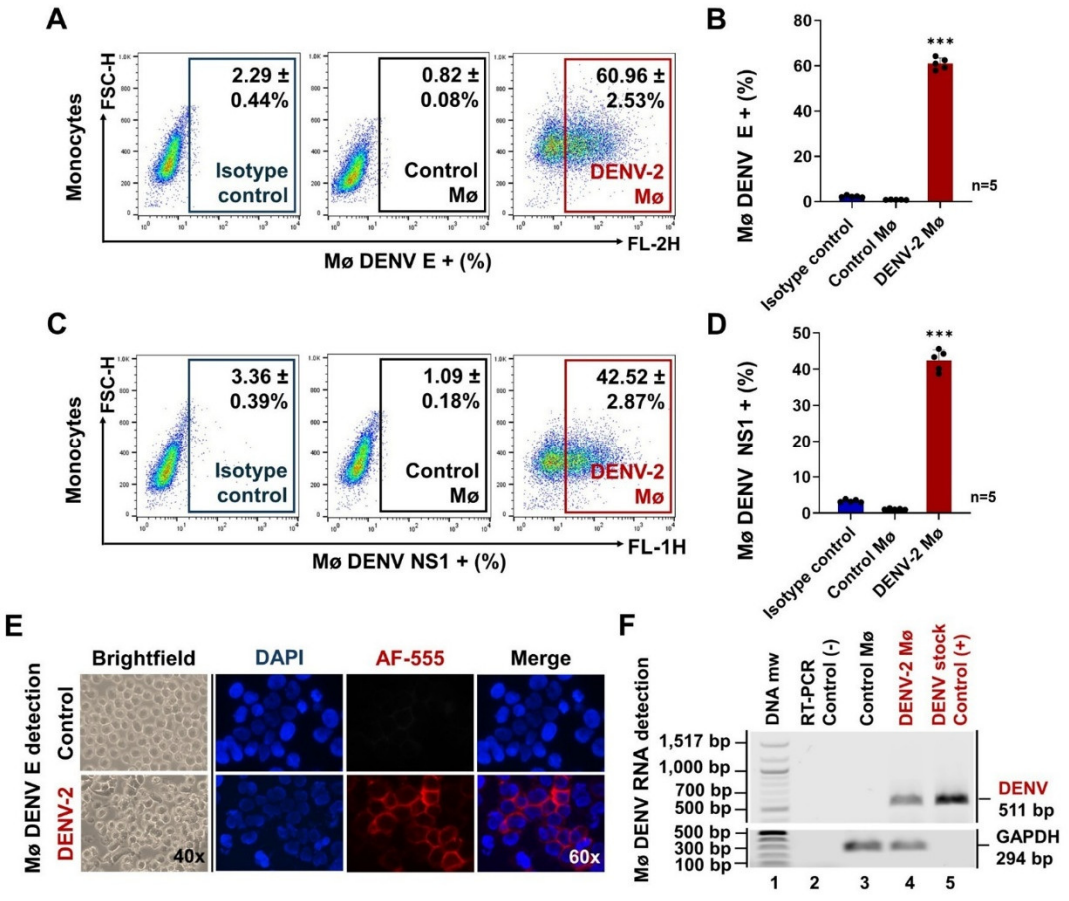

Figure 1. DENV-2 (MOI 1) infection in monocytes (Mø). (**A**) Detection of DENV E protein at 72 h p.i. (representative dot plots by FACS). (**B**) Percentages of E-positive Mø. (**C**) Detection of DENV NS1 protein at 72 h p.i. (representative dot plots by FACS). (**D**) Percentages of NS1-positive Mø. The percentages of Mø E+ and NS1+ from DENV-2 Mø were compared with Control Mø values using an unpaired Student's *t*-test. Statistical

 doi:10.20944/preprints202604.2219.v1

significance is denoted as *** when $p < 0.0001$. (**E**) Detection of the viral E protein (red) in DENV-infected monocytes by immunofluorescence microscopy (60×) at 72 h p.i. (**F**) Detection of DENV RNA by RT-PCR amplification in DENV-infected monocytes. Amplicons were visualized on 1.2% agarose gels stained with 2% ethidium bromide. Isotype control (blue), Control Mø (black), and DENV-2 Mø / DENV (red).

We confirmed the viral presence at 72 h p.i. through E protein immunostaining in DENV-infected Mø by fluorescence microscopy (Figure 1E), and by viral RNA amplification (511 bp amplicon corresponding to the conserved C/prM genomic region) from infected cell lysates (Figure 1F). A strong red signal associated with E protein expression in DENV-infected cells was observed, that was absent in Control Mø. In addition, the distinct DENV-specific amplicon band was detected in DENV-2 Mø samples, but not in Control Mø samples, indicating the presence of viral RNA within infected monocytes. These results demonstrate that our experimental model supports productive DENV infection and viral replication in monocytes, as evidenced by the detection of viral proteins and genomic RNA.

Monocytes are recognized as primary target cells for infection by different orthoflaviviruses and exhibit different levels of activation and differentiation [5–7]. Here, we evaluated the levels of CD14 (lipopolysaccharide [LPS] receptor), CD16 (Fc gamma receptor III), CD11b (integrin alpha M), and CD142 (Tissue Factor [TF] or coagulation factor III), as well as the mRNA expression of proinflammatory cytokine (TNF-α and IL-8), to assess the potential proinflammatory and procoagulant response (Figure 2).

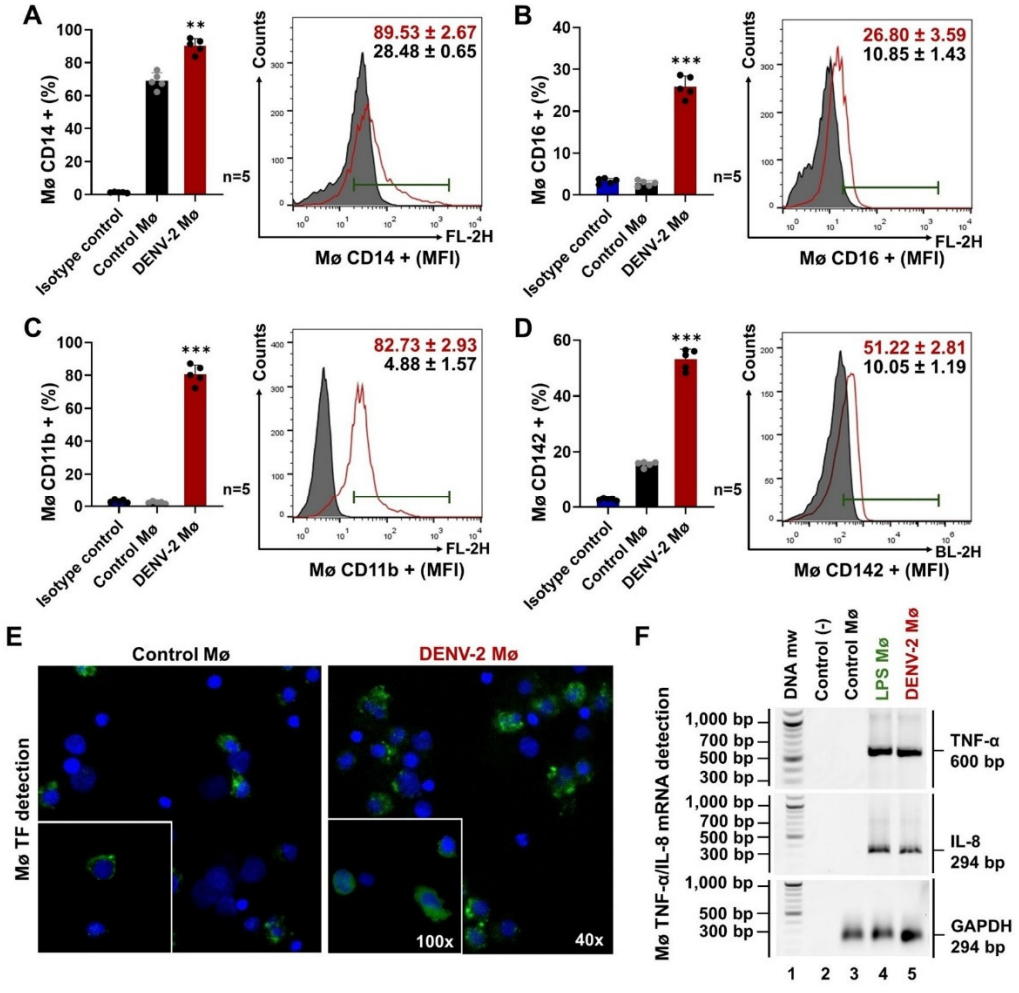

Figure 2. DENV infection promotes monocyte differentiation and proinflammatory/procoagulant activation. (**A**) Percentage of CD14+ monocytes (Mø) with a representative histogram showing mean fluorescence intensity

 doi:10.20944/preprints202604.2219.v1

(MFI) values obtained by FACS at 72 h p.i. (**B**) Percentage of CD16+ Mø with a representative histogram showing MFI values obtained by FACS at 72 h p.i. (**C**) Percentage of CD11b+ Mø with a representative histogram showing MFI values obtained by FACS at 72 h p.i. (**D**) Percentage of CD142+ Mø (Tissue Factor [TF] or coagulation factor III) with a representative histogram showing MFI values obtained by FACS at 72 h p.i. The percentages of CD14+, CD16+, CD11b+, and TF+ Mø from DENV-2 Mø were compared with Control Mø using an unpaired Student's *t*-test. Statistical significance is denoted as ** when $p < 0.001$ and *** when $p < 0.0001$. (**E**) Detection of TF (green) in monocytes by immunofluorescence microscopy (40× and 100×) at 72 h p.i. (**F**) Detection of proinflammatory cytokine mRNA (TNF-α and IL-8) by RT–PCR amplification in Mø. Amplicons were visualized on 1.2% agarose gels stained with 2% ethidium bromide. Isotype control (blue), Control Mø (black), Lipopolysaccharide (LPS)-stimulated Mø (dark green), and DENV-2 Mø (red).

Monocytes are classified into distinct populations based on CD14 and CD16 levels, namely classical, intermediate, and non-classical. Shifts in the distribution of these subsets reflect the establishment of an inflammatory state [6,7]. We evaluated CD14 and CD16 expression in response to DENV infection and found that, in uninfected cells (Control Mø), 69% (MFI = 28) and 3% (MFI = 11) of cells were CD14+ and CD16+ (Figure 2A–B), respectively, corresponding with the classical subset. In contrast, in DENV-infected Mø (DENV-2 Mø), 91% (MFI = 90) of cells were CD14+ and 26% (MFI = 27) were CD16+, indicating a shift toward the intermediate subset. The frequency of CD14+ and CD16+ monocytes increased by 1.3- ($p < 0.01$) and 9.3-fold ($p < 0.0001$), respectively, in DENV-2 Mø compared with Control Mø, suggesting that DENV infection promotes differentiation toward an intermediate, proinflammatory phenotype.

We also evaluated CD11b levels to further characterize monocyte activation (Figure 2C) and found that 81% (MFI = 83) of DENV-2 Mø were CD11b+ ($p < 0.0001$), whereas control Mø showed 2% (MFI = 5) of positivity, indicating that DENV infection enhances monocyte activation. Elevated CD11b is associated with increased monocyte adhesion capacity, facilitating interaction with the vascular endothelium [31].

Given the enhanced activation and adhesion profile of DENV-infected Mø, particularly the expansion of activated intermediate Mø, we assessed whether this phenotype is associated with the upregulation of TF protein (CD142), a key initiator of the coagulation cascade. DENV infection increased TF levels in monocytes by approximately 3-fold, from 16% (MFI = 10) in Control Mø to 53% (MFI = 51) in DENV-2 Mø ($p < 0.0001$) (Figure 2D). We confirmed these data by immunofluorescence microscopy, detecting a strong green signal in DENV-2 Mø samples consistent with TF presence (Figure 2E). The increased levels of TF suggest that, during DENV infection, activated intermediate Mø represent a source of circulating TF, thus contributing to coagulation activation and thrombus formation [32].

Considering the procoagulant phenotype observed in monocytes in response to DENV infection, characterized by the expansion of activated intermediate monocytes and increased TF expression, we evaluated whether this activation state is associated with a proinflammatory response by measure the mRNA expression of TNF-α and IL-8. Therefore, we analyzed lysates from Control Mø, LPS-stimulated Mø (LPS Mø; positive control), and DENV-2 Mø to assess proinflammatory cytokine expression by RT–PCR amplification. Distinct TNF-α and IL-8 amplicon bands in LPS Mø and DENV-2 Mø samples were observed, but not in Control Mø, supporting the transcriptional activation of proinflammatory cytokines. Although protein secretion was not quantified, the transcriptional detection of TNF-α and IL-8 provides initial molecular evidence that DENV infection promotes a proinflammatory response in activated intermediate monocytes.

These findings indicate that DENV infection drives a coordinated reprogramming of monocytes toward an activated intermediate phenotype with enhanced adhesion capacity and procoagulant and proinflammatory capabilities, providing a mechanistic framework to investigate their role in the generation of extracellular vesicles, particularly microparticles, and their potential contribution to vascular dysfunction described in severe dengue.

 doi:10.20944/preprints202604.2219.v1

2.2. DENV-Infected Monocytes Release Extracellular Vesicles (Microparticles), Carrying Viral Components that Promote Viral Dissemination to Endothelial Vascular Cells

Microparticles (MPs) are a subset of extracellular vesicles (EVs) released from activated cells through membrane budding, resulting from calcium-mediated disruption of cytoskeletal anchorage and loss of phospholipid asymmetry, whereby phosphatidylserine (PS) becomes externalized from the inner to the outer membrane leaflet, allowing MP release with PS exposed on the external surface [33,34]. Considering the differentiation and activation of DENV-infected monocytes in our experimental model, we evaluated the production of EVs (MPs) (Figure 3) to determine their possible function in DENV-associated vasculopathy.

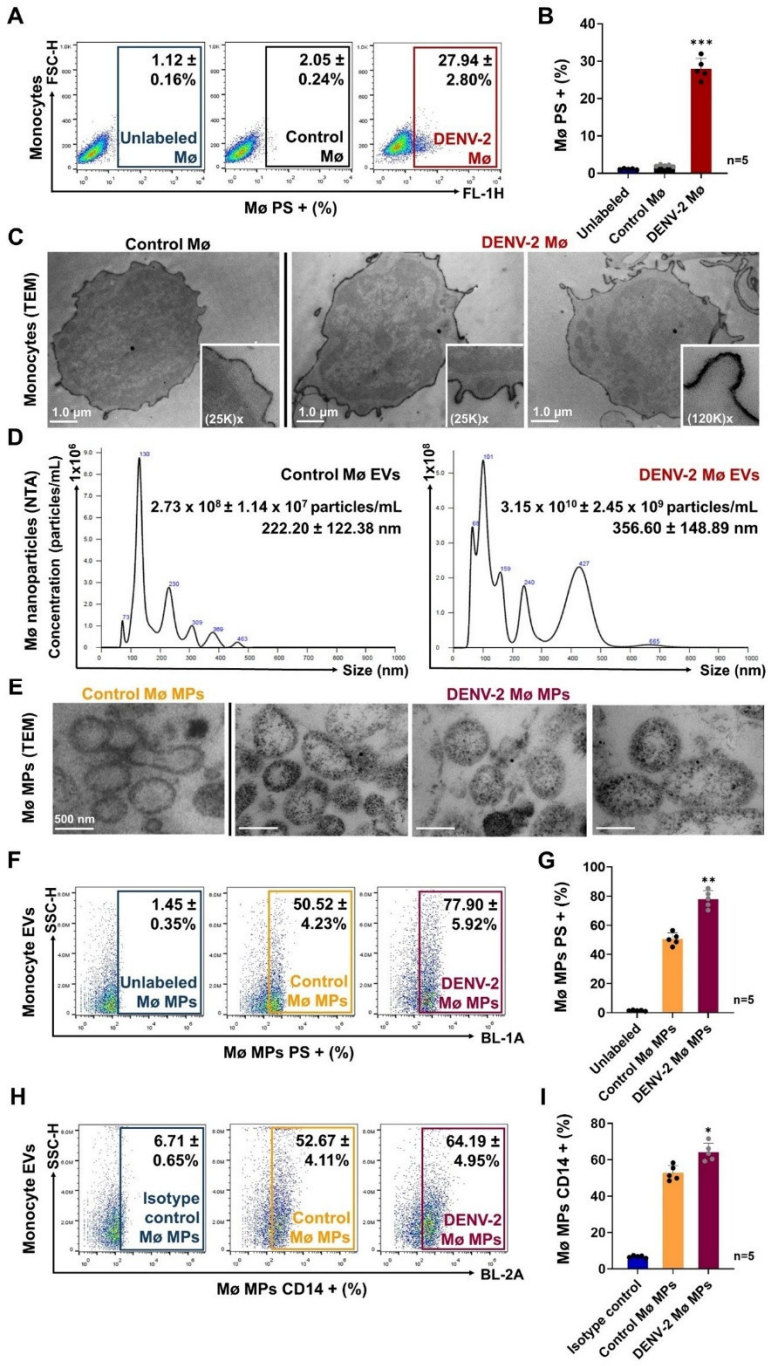

Figure 3. Characterization of extracellular vesicles (microparticles, MPs) released by monocytes. (**A**) Detection of phosphatidylserine (PS) by Annexin V binding assay at 72 h p.i. (representative dot plots by FACS). (**B**) Percentages of PS-positive monocytes (Mø). The percentage of Mø PS+ in DENV-2 Mø was compared with

 doi:10.20944/preprints202604.2219.v1

Control Mø using an unpaired Student's *t*-test. Statistical significance is denoted as *** when $p < 0.0001$. (**C**) Transmission electron microscopy (TEM) images of uninfected (Control Mø) and DENV-infected Mø (DENV-2 Mø) stained with ruthenium red (scale bar: 1.0 μm). (**D**) Nanoparticle tracking analysis (NTA) of monocyte-derived extracellular vesicles (Mø EVs). Representative histograms showing mean ± standard deviation of particle concentration (particles/mL) and size distribution from three independent experiments. (**E**) TEM images of MPs isolated from Control Mø and DENV-2 Mø (scale bar: 500 nm). (**F**) Detection of PS by Annexin V binding assay in Mø MP isolates at 72 h p.i. (representative dot plots by FACS). (**G**) Percentages of PS-positive MPs. (**H**) Detection of CD14 in Mø MP isolates at 72 h p.i. (representative dot plots by FACS). (**I**) Percentages of CD14-positive MPs. The percentages of Mø MPs PS+ and CD14+ from DENV-2 Mø MPs were compared with Control Mø MPs using an unpaired Student´s *t*-test. Statistical significance is denoted as * when $p < 0.05$ and ** when $p < 0.01$. Isotype control or unlabeled Mø (blue), Control Mø (black), DENV-2 Mø (red), Control Mø MPs (orange), and DENV-2 Mø MPs (cherry).

We evaluated PS exposure in the monocyte plasma membrane to determine whether DENV-2 Mø could release MPs at 72 h p.i. and found that 25% of DENV-2 Mø were PS+ ($p < 0.0001$), in contrast to Control Mø, where 2% of cells were PS+ (Figure 3A–B). Given that PS externalization at the plasma membrane can also be associated with dead cells, we assessed viable cell morphology by transmission electron microscopy (TEM) using ruthenium red staining, observing that DENV-2 Mø exhibited abundant membrane protrusions suggestive of active budding, consistent with MP release, whereas this was less evident in Control Mø (Figure 3C). These findings indicate that MPs may be generated relate to our experimental conditions and can be isolated for further characterization.

We adapted previously described protocols for EV isolation by differential ultracentrifugation from 1.0×10^7 monocytes (see Section 4.9, Materials and Methods). The EV fractions corresponding to MP pellets were characterized by nanoparticle tracking analysis (NTA) to determine particle concentration and size distribution. We found that DENV-2 Mø released approximately 3.15×10^{10} particles/mL, with a mean size of 357 nm, representing 1.2- and 1.6-fold increases in concentration and size, respectively, compared with Control Mø samples (Figure 3D). Morphologically, TEM images showed heterogenous populations of large EVs with well-defined lipid bilayers and size consistent with MPs. In DENV-2 Mø-derived MPs (DENV-2 Mø MPs), we observed irregular and electron-dense internal structures, which were absent in Control Mø-derived MPs (Control Mø MPs) (Figure 3E).

The monocyte membrane origin of EVs was evaluated in MP isolates by detecting PS and CD14 at surface membrane level by FACS. For DENV-2 Mø MP isolates, 78% were PS+ and 64% were CD14+, representing 1.5- ($p < 0.01$) and 1.1-fold ($p < 0.05$) increases in the levels of PS and CD14, respectively, compared with Control Mø MPs (Figure 3F–I). These data confirm that the EV fractions isolated from monocytes are predominantly composed of MPs.

The present results demonstrate that DENV-infected intermediate monocytes actively release MPs, as evidenced by increased PS externalization, enhanced membrane budding, and the recovery of EV fractions with size and morphology consistent with MPs. These EVs exhibit characteristic surface markers, including PS and CD14, confirming their monocyte membrane origin because of infection-induced activation. Notably, DENV infection significantly increased both the production and structural complexity of MPs, suggesting that these vesicles may serve as biologically carriers in the context of infection. Therefore, we evaluated whether DENV-2 Mø-derived MPs transport viral components like the E and NS1 proteins, and whether this capability may contribute to viral transmission and facilitate endothelial vascular cells infection, potentially predisposing the vascular endothelium to dysfunction and damage (Figure 4).

Preprints.org (www.preprints.org) | NOT PEER-REVIEWED | Posted: 30 April 2026 doi:10.20944/preprints202604.2219.v1

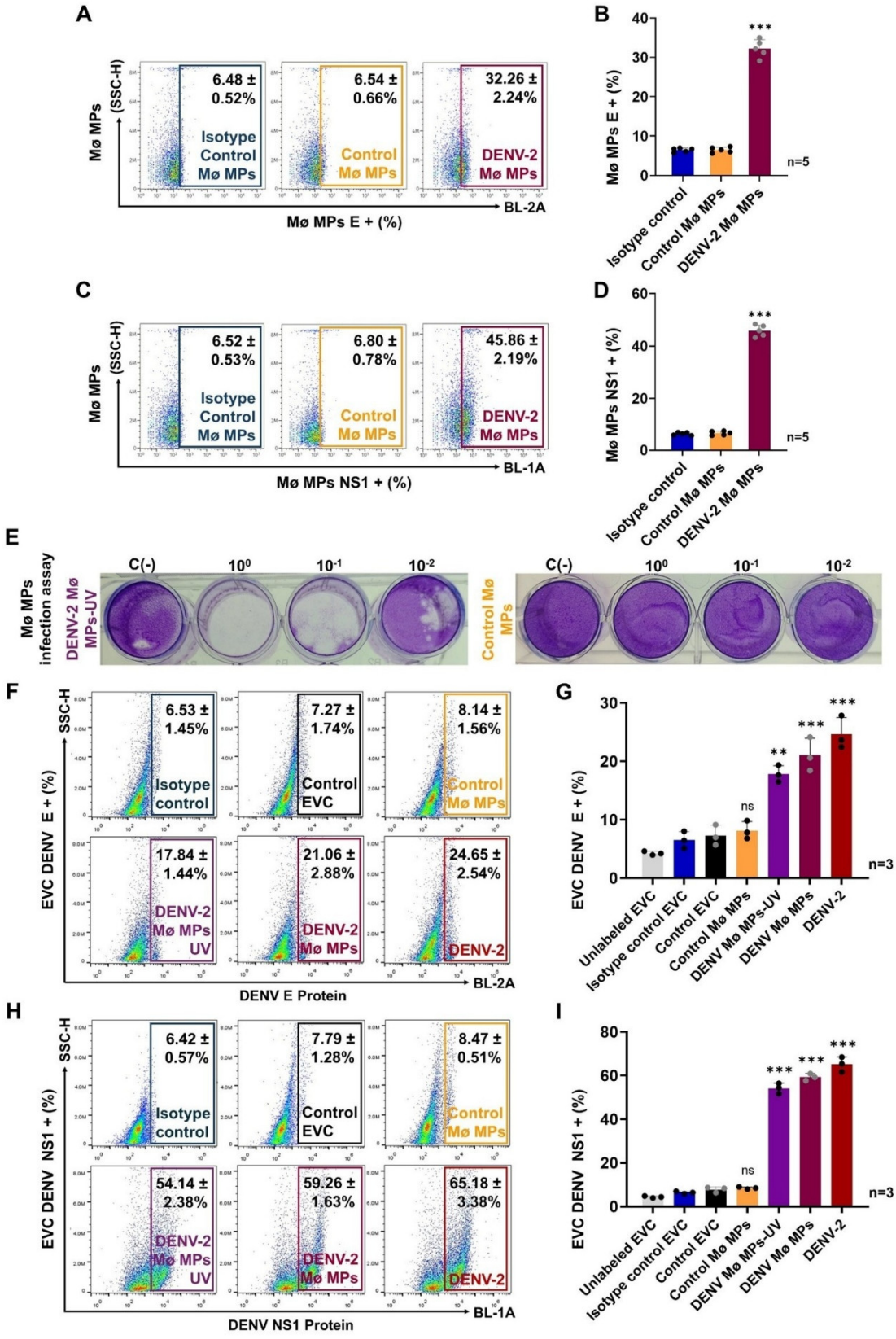

Figure 4. DENV-infected intermediate monocyte-derived MPs carry viral components and promote infection of endothelial vascular cells (EVC). (**A**) Detection of DENV E protein in Mø MP isolates at 72 h p.i. (representative dot plots by FACS). (**B**) Percentage of E-positive MPs. (**C**) Detection of DENV NS1 protein in Mø MP isolates at 72 h p.i. (representative dot plots by FACS). (**D**) Percentage of NS1-positive MPs. The percentages of E+ and NS1+ MPs from DENV-2 Mø MP isolates were compared with Control Mø MP isolates using an unpaired

 doi:10.20944/preprints202604.2219.v1

Student's *t*-test. (**E**) Representative images of lytic plaque assays performed on Vero cells stimulated with DENV-2 Mø-derived MPs-UV and Control Mø-derived MPs. (**F**) Detection of DENV E protein in EVC stimulated with Mø MP isolates at 72 h post-stimulation. (**G**) Percentage of E+ EVC. (**H**) Detection of DENV NS1 protein in EVC stimulated with Mø MP isolates at 72 h post-stimulation. (**I**) Percentage of NS1+ EVC. The percentages of E+ and NS1+ EVC under different Mø MP stimuli were compared with Control EVC (uninfected cells) using a one-way ANOVA test. Statistical significance is denoted as ** when $p < 0.01$ and *** when $p < 0.0001$; ns = not significant. Unlabeled cells (light gray), Isotype control (blue), Control EVC (black), Control Mø MPs (orange), DENV-2 Mø MPs-UV (purple), DENV-2 Mø MPs (cherry), and DENV-2 (red).

We found that 32% of DENV-2 Mø-derived MPs presented viral E protein at membrane surface level, which was absent in Control Mø-derived MPs ($p < 0.0001$) (Figure 4A–B). DENV-infected Mø-derived MPs may acquire viral content like the E protein during membrane budding concomitant with virion release, allowing them to carry viral material within their internal content, or through virus–MP membrane interactions in the extracellular space [35–38]. Regardless of the underlying mechanism, DENV-infected Mø-derived MPs may contribute to viral dissemination by facilitating infection of naïve cells that interact with these vesicles.

Importantly, we found that 46% of DENV-2 Mø-derived MPs shown viral NS1 protein at membrane surface, whereas NS1 was not detected in Control Mø-derived MPs ($p < 0.0001$) (Figure 4C–D). DENV NS1 protein is a key virulence factor implicated in vascular dysfunction through different mechanisms like glycocalyx degradation, disruption of intercellular junctions, and induction of acute inflammatory response that ultimately compromise vascular barrier integrity [39]. It has been reported that NS1 remains in a dimeric form in DENV-infected cells and is released in a multimeric form to the extracellular space [40], which could be acquired by EVs like exosomes [41]. This data is particularly relevant in the context of DENV-associated vasculopathy, as MPs also may function as circulating carriers of NS1, enabling its delivery to endothelial vascular cells and plausibly amplifying vascular activation and tissue damage.

Together, these findings indicate that DENV-infected Mø-derived MPs carry viral E and NS1 proteins, supporting their potential role as carriers of pathogenic viral components and sustain a mechanism basis to evaluate their capacity to mediate viral transmission and to induce functional alterations in target cells.

To determine the capacity of DENV-infected Mø-derived MPs to mediate viral transmission, we adapted a lytic plaque assay protocol (see Section 4.3, Materials and Methods) to evaluate plaque formation in confluent Vero cell monolayers following stimulation with MP isolates. MP-containing fractions were obtained through a low-speed centrifugation step during EV isolation, a condition under which large vesicles such as MPs are pelleted while virions are expected to remain in the supernatant. To further minimize potential contamination with free virions or viral RNA, MP isolates were washed twice with 1× PBS prior to UV inactivation. These steps ensured that the observed infectivity was primarily associated with MP-bound viral material. We observed that stimulation with UV-inactivated DENV-infected Mø-derived MPs (DENV-2 Mø MPs-UV) induced the formation of lytic plaques, suggesting active infection mediated by MP-associated viral components, which was not observed upon stimulation with Control Mø-derived MPs (Figure 4E).

We previously reported [42] that DENV infection of endothelial vascular cells (EVC) directly promotes vasculopathy through active viral replication, leading to high levels of viremia and the activation of intracellular signaling pathways that favor vascular activation, tissue damage, and increased permeability of endothelial vascular barrier. However, viral infection may also occur through alternative mechanisms, whereby infectious viral components (RNA or complete virions) can reach target cells in a receptor-independent manner. In this context, EVs may function as Trojan horses, facilitating viral transmission and active infection. Therefore, we performed stimulation assays with different Mø MP isolates in naïve EVC to determine their potential role in viral dissemination by detecting E and NS1 proteins at the endothelial cell membrane surface.

 doi:10.20944/preprints202604.2219.v1

We found that 18% of EVC incubated with DENV-Mø MPs-UV were E+ ($p < 0.01$), whereas 21% of EVC stimulated with DENV-Mø MPs and 25% of EVC infected with DENV-2 (MOI 1) were E+ ($p < 0.0001$). E protein was not detected in control EVC or in cells cultivated with Control Mø MPs (Figure 4F–G), suggesting that MP-associated viral infectious content facilitates cellular infection. In parallel, 54% of EVC stimulated with DENV-Mø MPs-UV were NS1+ ($p < 0.0001$), whereas 59% of EVC stimulated with DENV-Mø MPs and 65% of EVC infected with DENV-2 (MOI 1) were NS1+ ($p < 0.0001$). NS1 protein was not detected in Control EVC or in Control Mø MPs-stimulated cells (Figure 4H–I). These data support that DENV-2-infected Mø-derived MPs facilitate viral transmission by the interaction with naïve EVC. The presence of E protein together with the high abundance of NS1 suggests that EVC undergoes acute infection associated with an active DENV replication cycle. Moreover, the presence of NS1 indicates that EVC may be susceptible to NS1-mediated injury and/or host inflammatory response.

Then, our results demonstrate that DENV infection induces a functional reprogramming of monocytes that promotes the release of MPs, which carry both infectious and pathogenic viral components (NS1). DENV-Mø MPs, could mediate viral infection, as evidenced by lytic plaque formation in Vero cells, even after UV inactivation, indicating a protected and transmissible viral cargo. Moreover, MPs derived from DENV-infected Mø facilitated the transfer of viral components to endothelial vascular cells, promoting their infection and suggesting the establishment of an active viral replication cycle. In parallel, the presence of NS1 focuses on a potential mechanism by which these vesicles may contribute to vascular dysfunction and damage. Together, these results support a model in which monocyte-derived MPs act as Trojan-like vehicles that enhance viral dissemination and favor endothelial vascular cells injury as present in severe dengue cases.

2.3. DENV-Infected Mø-Derived MPs Exhibit Procoagulant Activity and Promote Vascular Dysfunction and Endothelial Vascular Barrier Disruption

Dengue-associated vasculopathy is characterized by functional and structural alterations in the vascular endothelium induced by DENV infection, leading to a shift toward a procoagulant, proinflammatory, and proadherent phenotype in EVC, ultimately resulting in endothelial vascular cell damage, increased permeability, and plasma leakage [4,43]. Vasculopathy, as a pathognomonic sign of severe dengue, results from the convergence of multiple factors, including viral serotype, high viral load, antibody-dependent enhancement, platelet activation, and the release of proinflammatory mediators; however, its underlying mechanisms remain incompletely understood [44,45].

Our data show that DENV-infected Mø-derived MPs carry both structural (E) and non-structural (NS1) viral proteins and promote viral transmission and active infection in EVC, potentially predisposing the vascular endothelium to damage through the accumulation of NS1 at the cell surface. Considering that these MPs originate from activated intermediate Mø with a TF+ phenotype and are enriched in PS, we evaluated their procoagulant potential by assessing TF presence at membrane surface and their capacity to generate thrombin, as well as their contribution to vascular endothelium dysfunction (Figure 5).

 doi:10.20944/preprints202604.2219.v1

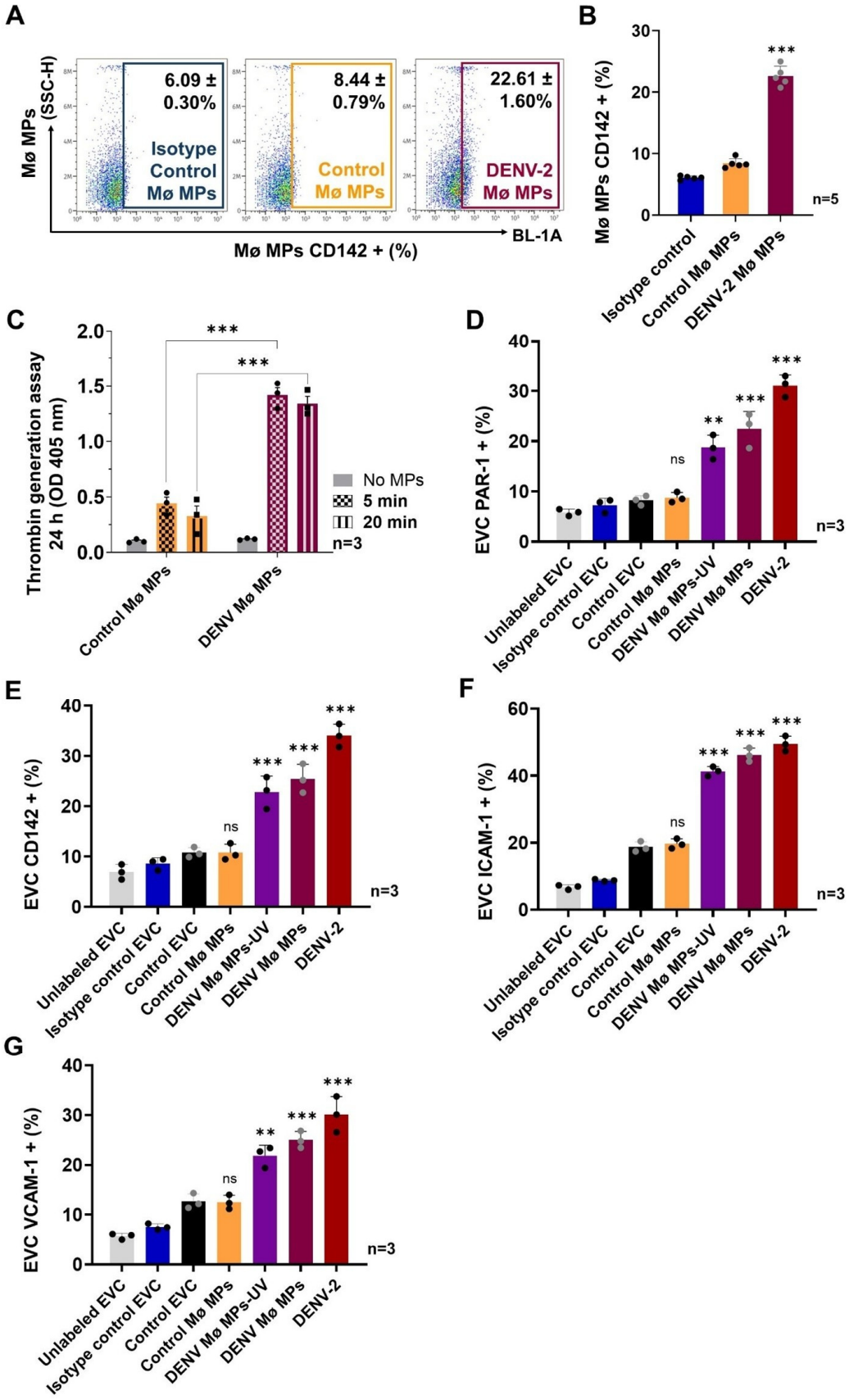

Figure 5. Procoagulant DENV-2 Mø-derived MPs promote a shift toward a procoagulant, proinflammatory, and proadherent phenotype in EVC. (**A**) Detection of TF (CD142) in Mø MP isolates at 72 h p.i. (representative dot plots by FACS). (**B**) Percentage of TF+ MPs. The percentage of TF+ MPs from DENV-2 Mø MP isolates was compared with Control Mø MP isolates using an unpaired Student's *t*-test. (**C**) Thrombogenicity assay using Mø

 doi:10.20944/preprints202604.2219.v1

MP isolates at 24 h post-incubation. Thrombin generation time (5 and 20 min) was analyzed using a two-way ANOVA test. (**D**) Percentage of PAR-1+ EVC stimulated with Mø MP isolates at 72 h post-stimulation. (**E**) Percentage of TF+ EVC stimulated with Mø MP isolates at 72 h post-stimulation. (**F**) Percentage of ICAM-1 (CD54)+ EVC stimulated with Mø MP isolates at 72 h post-stimulation. (**G**) Percentage of VCAM-1 (CD106)+ EVC stimulated with Mø MP isolates at 72 h post-stimulation. The percentages of PAR-1, TF+, ICAM-1+, and VCAM-1+ EVC under different Mø MP stimuli were compared with Control EVC (uninfected cells) using a one-way ANOVA test. Statistical significance is denoted as ** when $p < 0.01$ and *** when $p < 0.0001$; ns = not significant. Unlabeled cells (light gray), Isotype control (blue), Control EVC (black), Control Mø MPs (orange), DENV-2 Mø MPs-UV (purple), DENV-2 Mø MPs (cherry), and DENV-2 (red).

We found that 32% of DENV-2 Mø-derived MPs were TF+ ($p < 0.0001$), whereas 7% of Control Mø-derived MPs were TF+, representing a 4.6-fold increase (Figure 5A–B). This finding suggests that DENV-2 Mø-derived MPs may act as a source of circulating TF and anionic phospholipids (PS) (Figure 3F–G), thereby contributing to activation of the coagulation cascade.

To assess their functional procoagulant activity, we evaluated the thrombin generation capacity of DENV-2 Mø-derived MPs using a colorimetric assay based on thrombin enzymatic activity on a chromogenic substrate at different time points (Figure 5C; see Section 4.15, Materials and Methods). We found that DENV-2 Mø-derived MPs promoted thrombin generation by approximately 3.0-fold more, compared with Control Mø-derived MPs at 24 h post-incubation, using platelet-poor plasma as a source of coagulation factors. The peak enzymatic activity was detected at 5 min after substrate addition ($p < 0.0001$), supporting their capacity to activate the coagulation cascade and promote a prothrombotic state.

These results indicate that DENV-2 Mø-derived MPs contain functional procoagulant elements (PS+ TF+) which may contribute to the establishment of a prothrombotic activity during progression to coagulopathy and potentially as an active actor in the development of disseminated intravascular coagulation (DIC) as present in severe dengue cases [43].

Based on our previous findings that DENV-2 Mø-derived MPs carry viral components and promote viral transmission and active infection in endothelial vascular cells, underlining that these MPs transport NS1, a key virulence factor known to induce vascular dysfunction. Together with their procoagulant capacity, these MPs may enhance thrombin generation at the endothelial interface. This convergence of viral and coagulation-dependent mechanisms suggests that DENV-2 Mø-derived MPs act as multifunctional effectors of vascular activation and damage.

Given their capacity to generate thrombin, DENV-2 Mø-derived MPs may directly influence endothelial vascular cells activation. Thrombin is a key effector of the coagulation cascade that activates endothelial vascular cells through protease-activated receptor (PAR-1) signaling, promoting inflammatory responses, expression of adhesion molecules, and a procoagulant phenotype [42,46]. Therefore, we assessed whether stimulation of EVC with DENV-2 Mø-derived MPs induces PAR-1, TF, and proadherent molecules [intercellular adhesion molecule type 1 (ICAM-1) and vascular cell adhesion molecule type 1 (VCAM-1)] expression, to establishing a mechanistic link between MP-induced thrombin generation and vascular dysfunction characteristic of DENV-associated vasculopathy.

In a procoagulant and prothrombotic environment, the presence and/or upregulation of PAR-1 in endothelial vascular cells reflects their ability to sense and respond to thrombin and other coagulation proteases, thereby mediating the crosstalk between coagulation and inflammation, including the induction of proinflammatory cytokine signaling [42,47].

In response to stimulation with DENV-2 Mø MPs-UV, 19% of EVC were PAR-1+, representing an approximately 2.4-fold increase compared with Control EVC and Control Mø MPs-stimulated EVC ($p < 0.01$). PAR-1 levels further increased in EVC stimulated with DENV-2 Mø MPs (22%) and in DENV-2-infected EVCs (31%) ($p < 0.0001$) (Figure 5D). This data supports that DENV-2 Mø MPs may have a role as mediators of thrombin-responsive signaling pathways. This upregulation of PAR-1 suggests that procoagulant DENV-2 Mø-derived MPs may sensitize EVC to coagulation proteases,

 doi:10.20944/preprints202604.2219.v1

thereby amplifying proinflammatory and procoagulant responses, contributing to vascular activation and dysfunction.

Consistent with the activation of thrombin-responsive signaling pathways mediated by PAR-1, we next evaluated whether this response translates into a procoagulant vascular endothelium phenotype, as shown by increased TF levels. We found that 23% of EVC stimulated with DENV-2 Mø MPs-UV were TF+, representing an approximately 2.1-fold increase compared with Control EVC and Control Mø MPs-stimulated EVC ($p < 0.0001$). As controls, 25% of EVC stimulated with DENV-2 Mø MPs and 34% of DENV-2-infected EVC were TF+, respectively ($p < 0.0001$) (Figure 5E). This finding suggests that DENV-2 Mø MPs are potent enhancers of a procoagulant endothelium phenotype.

Our results indicate that DENV-2 Mø MPs induce procoagulant and proinflammatory EVC phenotypes characterized by increased PAR-1 and TF levels. This response suggests that MP-driven thrombin generation not only enhances vascular endothelium sensitivity to coagulation proteases but also promotes a sustained activation state that may amplify local coagulation, inflammation and EVC dysfunction.

As this activated phenotype is closely linked to vascular inflammation and leukocyte adhesion, we evaluate if DENV-2 Mø-derived MPs promote the presence of the proadherent molecules ICAM-1 and VCAM-1 in EVC.

We found that 41% and 22% of EVC stimulated with DENV-2 Mø MPs-UV were ICAM-1+ and VCAM-1+, respectively, representing an approximately 2.1-fold increase for ICAM-1 and 1.7-fold increase for VCAM-1 compared with Control EVC and Control Mø MPs-stimulated EVC ($p < 0.0001$). In EVC stimulated with DENV-2 Mø MPs, 46% of cells were ICAM-1+ and 25% were VCAM-1+, whereas in DENV-2-infected EVC, 50% and 30% of cells were ICAM-1+ and VCAM-1+, respectively (Figure 5F–G). These results indicate that DENV-2-infected Mø-derived MPs promote endothelium activation toward a proinflammatory and proadherent phenotype, favoring leukocyte adhesion (e.g., intermediate monocytes) and suggesting a compromised vascular endothelial cells barrier that may contribute to vascular leakage.

We have demonstrated that DENV-2 Mø-derived MPs (PS+ NS1+ TF+) promote vascular endothelium activation characterized by procoagulant, proinflammatory, and proadherent responses, features consistent with DENV-associated vasculopathy. Therefore, we evaluated whether stimulation with these Mø MPs compromises endothelial barrier integrity. Increased endothelial vascular permeability is a hallmark of severe dengue and reflects disruption of endothelial junctions and alteration of vascular barrier function [43]. In this context, we assessed if exposure to DENV-2 Mø-derived MPs induces changes consistent with vascular barrier dysfunction using Transwell assays (Figure 6).

 doi:10.20944/preprints202604.2219.v1

A

Endothelial permeability assay							
Tested conditions							
Number of cells (cells/mL)	Transwell pore size (µm)	Cell growth time (h)	LPS (mg/mL)	DENV (MOI)	MPs (mg/mL)	FITC-Dextran (kDa)	FITC-Dextran incubation time (h)
2.0×10^5, 2.5×10^5, 3.0×10^5, 3.5×10^5	0.4, 1	24, 48, 72	0.5, 1.0	1, 5	0.5, 1.0	4, 40	1, 3
Experimental conditions							
3.5×10^5	0.4	48	1.0	1	1.0	40	1

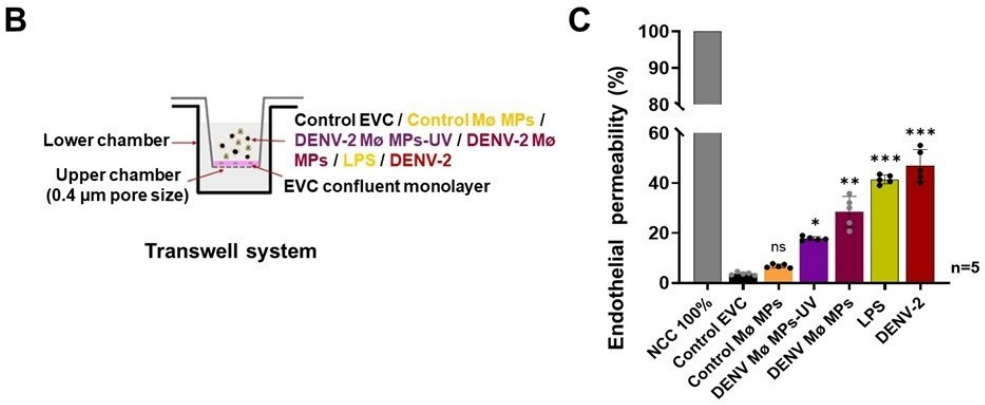

Figure 6. DENV-2-infected Mø-derived MPs increase vascular permeability in EVC. (**A**) Overview of the tested conditions and the experimental parameters established for the EVC permeability assay. (**B**) Schematic representation of the Transwell system used for the EVC permeability assay. (**C**) Endothelial permeability percentages were determined by measuring fluorescein isothiocyanate (FITC)-dextran that crossed EVC monolayers following stimulation with Mø MP isolates. For 100% permeability, a FITC-dextran–only control (no-cell control, NCC) was used. Permeability percentages were compared with Control EVC using a one-way ANOVA test. Statistical significance is denoted as * when $p < 0.05$, ** when $p < 0.01$, and *** when $p < 0.0001$; ns = not significant. NCC 100% (dark gray), Control EVC (black), Control Mø MPs (orange), DENV-2 Mø MPs-UV (purple), DENV-2 Mø MPs (cherry), LPS (dark yellow), and DENV-2 (red).

First, we established the optimal conditions for the permeability assay (Figure 6A–B), in which fluorescence from FITC-dextran crossing the Transwell membrane was measured to calculate endothelial vascular cells permeability percentages (p%). We found that stimulation with DENV-2 Mø-derived MPs increased EVC permeability, with p% values of 4% in Control EVC, 7% in EVC stimulated with Control Mø MPs, 18% in EVC stimulated with DENV-2 Mø MPs-UV ($p < 0.05$), 29% in EVC stimulated with DENV-2 Mø MPs ($p < 0.01$), 42% in LPS-stimulated EVC, and 47% in DENV-infected EVC ($p < 0.001$) (Figure 6C). The permeability induced by DENV-2 Mø MPs-UV represented a 4.5- and 2.6-fold increase compared with Control EVC and EVC stimulated with Control Mø MPs, respectively. These data demonstrate that DENV-2-infected Mø-derived MPs promote endothelial barrier dysfunction, leading to increased vascular permeability, a key feature of DENV-associated vasculopathy.

The present data supports that DENV-2 infected monocytes favor functional cells modifications that promote the release of microparticles, carrying both viral components and procoagulant determinants. The DENV-infected Mø-derived MPs (PS+, TF+, E+/NS1+) act as multifunctional effectors that favor viral dissemination with coagulation and inflammatory responses. Functionally, these vesicles promote thrombin generation and activate endothelial vascular cells, inducing a procoagulant, proinflammatory, and proadherent phenotype characterized by increased levels of PAR-1, TF, ICAM-1, and VCAM-1. This activated state ultimately compromises endothelial barrier integrity, leading to increased vascular barrier permeability, a hallmark of DENV-associated vasculopathy. Together, these results support a mechanistic model in which monocyte-derived MPs

 doi:10.20944/preprints202604.2219.v1

contribute to the amplification of vascular dysfunction during DENV infection, highlighting their relevant role in the pathogenesis of severe dengue.

3. Discussion

The incidence of dengue fever (DF) has increased significantly worldwide in recent decades. About half of the world's population is at risk of DENV infection [1,3]. The main impacts of DF are on human health and national/global economies. Severe dengue (SD) is a cause of serious illness and death, mainly in Asia and Latin America. At present, no safe vaccine or specific treatment for DENV infection is available. The pathogenesis of SD is characterized by high viremia levels (low rate of viral clearance), increased endothelial vascular cells (EVC) activation, the enhanced production of proinflammatory cytokines, increased vascular permeability, plasma extravasation, and EVC damage. The vascular endothelium plays a determining role in the response to injury because it functions as a regulatory interface during hemostasis (coagulation–fibrinolysis–inflammation) and as a key regulator of endothelial barrier integrity [48]. During DENV infection, EVC, monocytes, and immune cells are the major targets affected by direct and/or indirect mechanisms. In this context, EVC dysfunction is strongly related to the clinical outcomes [44,49].

We previously reported that DENV infection of human EVC upregulates TF, triggering the generation of hemostatic proteases (thrombin) that induce the activation of PAR with the subsequent signaling inflammatory pathway, supporting the upregulation of adhesion (VCAM-1) or pro-inflammatory (IL-8) molecules as part of the pathogenic mechanisms for dengue-associated vasculopathy [42]. However, it is currently unknown whether microparticles derived from viral target cells like monocytes may contribute to the pathogenic mechanisms associated with SD, which involves three main factors: i.e., multiple defects in the coagulation–inflammation process, increased vascular permeability with plasma extravasation or endothelial dysfunction, which may progress to shock, multiorgan failure, and death [37,50,51].

Our findings demonstrate that DENV monocytes infection induces a functional reprogramming toward an activated intermediate phenotype with proinflammatory and procoagulant elements, leading to the release of EVs, predominantly MPs. These DENV-infected Mø-derived MPs (PS+, TF+, and viral E+/NS1+) act as multifunctional effectors that integrate viral dissemination with coagulation and inflammatory pathways. As well, we found that these vesicles transport viral components capable of mediating endothelial infection and DENV dissemination, while simultaneously exhibiting a procoagulant profile that promotes thrombin generation and activation of thrombin-responsive signaling pathways in endothelial vascular cells.

At vascular endothelium level, DENV-infected Mø MPs interaction induces a shift toward a procoagulant, proinflammatory, and proadherent phenotype, characterized by increased expression of PAR-1, TF, ICAM-1, and VCAM-1, reflecting the establishment of a sustained activation state. This functional alteration in due course compromises vascular barrier integrity, leading to increased vascular permeability, a hallmark of DENV-associated vasculopathy and a central event in the progression to severe dengue (Figure 7).

 doi:10.20944/preprints202604.2219.v1

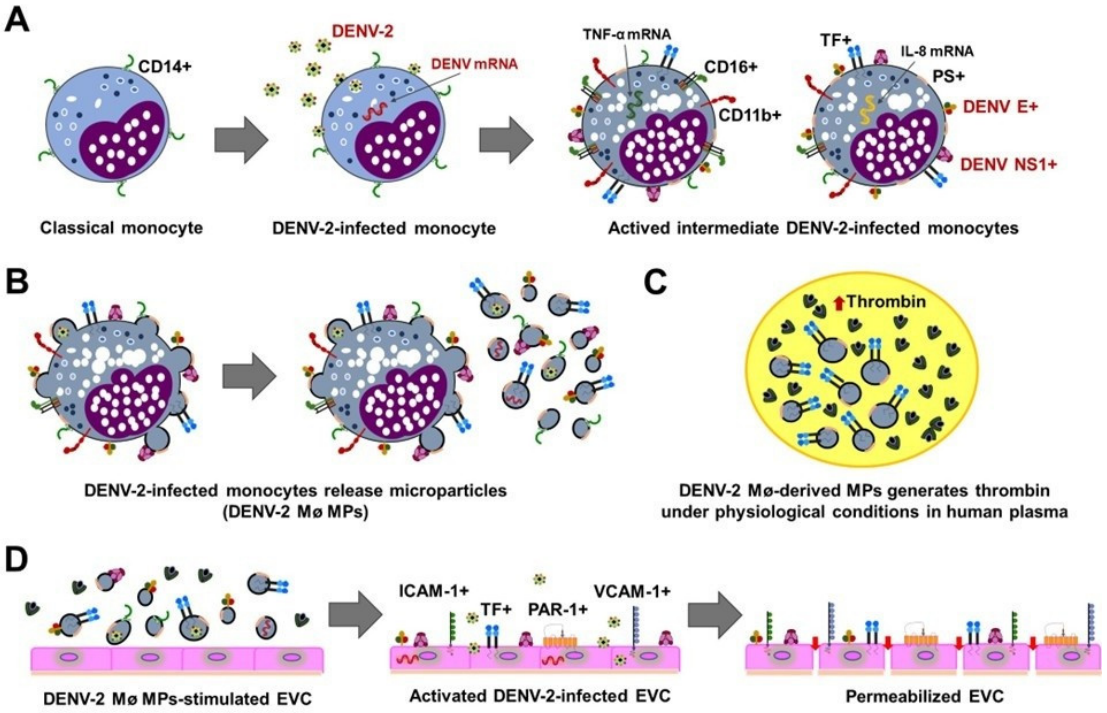

Figure 7. Microparticles from dengue virus-infected monocytes mediate endothelial vascular cells (EVC) infection and promote procoagulant and proinflammatory responses leading to increased barrier permeability (Graphical overview). (**A**) DENV infection induces functional reprogramming of monocytes toward an activated intermediate phenotype with proinflammatory and procoagulant features. (**B**) Activated intermediate DENV-infected monocytes release microparticles CD14+, PS+, TF+ carrying viral E and NS1 proteins. (**C**) Microparticles derived from DENV-infected monocytes exhibit a procoagulant profile (TF+ PS+) that promotes thrombin generation. (**D**) Upon interaction with EVC, microparticles derived from DENV-infected monocytes favor infection and induce a shift toward a procoagulant, proinflammatory, and proadherent phenotype, ultimately compromising barrier integrity and leading to increased vascular permeability.

Together, these findings support a model for the study in which DENV infected monocyte-derived MPs contribute to the amplification of vascular dysfunction during DENV infection, acting as intermediaries that associate viral spread with host-derived pathogenic responses.

From a translational perspective, these results highlight the potential of monocyte MPs as both biomarkers of disease severity and targets for therapeutic intervention, particularly in the context of endothelial dysfunction and dysregulated coagulation. Further characterization of MP-associated cargo and signaling pathways may provide new insights into host–virus interactions that underlie the progression to the severe forms of the disease.

Although these findings were generated using *in vitro* models, which may not fully recapitulate the complexity of the in vivo environment, they provide a controlled framework to dissect cellular and molecular mechanisms that are difficult to isolate in human disease. Notably, the lack of animal models that faithfully reproduce the full spectrum of SD pathogenesis in humans underscores the value of these experimental studies for the elucidation of the mechanisms involved in the tissue injury process. In this context, our data may be interpreted as evidence of biologically plausible pathways during endothelial vascular cells DENV damage. Importantly, while DENV-infected Mø MPs do not exceed DENV in their intrinsic infectivity, our findings support their role as complementary mediators that facilitate and may enhance viral dissemination and amplify host responses associated with vascular dysfunction. Therefore, microparticles derived from DENV-infected monocytes should be considered as relevant contributors to disease progression that warrant further investigation in more complex biological systems. Likewise, this another possibility dissemination mechanism may contribute to understanding viral persistence and pathogenesis by infecting distal or less-permissive

 doi:10.20944/preprints202604.2219.v1

cells. EVs-mediated viral spread provides foundational insights into DENV virulence and identifies as potential therapeutic targets to disrupt viral dissemination.

4. Materials and Methods

4.1. Cell Cultures

Monkey kidney epithelial cells (Vero; ATCC CCL-81, USA) and human peripheral blood monocytes THP-1 (ATCC TIB-202) were cultured in Dulbecco's Modified Eagle Medium (DMEM; Biowest, Riverside, MO, USA) and RPMI-1640 medium (Biowest), respectively. Both media were supplemented with 10% (v/v) fetal bovine serum (FBS; Biowest), 2 mM L-glutamine (Biowest), and a standard antibiotic–antimycotic mixture (1×) containing 100 U/mL penicillin, 0.1 mg/mL streptomycin, and 0.25 µg/mL amphotericin B (Biological Industries, Cromwell, CT, USA).

Human microvascular endothelial cells (HMEC-1; ATCC CRL-3243) were maintained in MCDB 131 medium (Sigma-Aldrich, St. Louis, MO, USA) supplemented with 10% FBS, 2 mM L-glutamine, 1× antibiotic–antimycotic solution, 10 ng/mL epidermal growth factor (Sigma-Aldrich), and 1 µg/mL hydrocortisone (Sigma-Aldrich). All cell cultures were incubated at 37 °C in a humidified atmosphere containing 5% CO_2.

4.2. Isolation, Propagation and Purification of Dengue Virus

The prototype dengue virus serotype 2 strain New Guinea C (DENV-2 NGC) was used throughout the study. Viral stocks were propagated in confluent Vero cell monolayers at a multiplicity of infection (MOI) of 0.5 and maintained at 37 °C with 5% CO_2 for 7 days. Culture supernatants were harvested and clarified by low-speed centrifugation (GH3.8 rotor, Beckman GPR Centrifuge; Beckman Coulter, Inc., Brea, CA, USA) at 200× g for 15 minutes (min) at room temperature (rt) to remove cellular debris.

Clarified DENV-2 was concentrated by precipitation with 10% polyethylene glycol 8000 with 15% NaCl and further purified by ultracentrifugation on a discontinuous sucrose gradient (5–50%, w/v) using an SW28 rotor in a Beckman XL-90 ultracentrifuge (Beckman Coulter, Inc.) at 120,000× g for 2 hours (h) at 4 °C. Purified viral fractions were collected, aliquoted, and stored at −72 °C until use.

4.3. Titration of DENV-2 Stock

Confluent Vero cell monolayers grown in 12-well culture plates (Corning, NY, USA) were infected with 450 µL of 10-fold serial dilutions of the DENV-2 stock in duplicate and incubated for 2 h at 37 °C with 5% CO_2 to allow viral adsorption. Following adsorption, the inoculum was removed and cells were overlaid with DMEM supplemented with 1% carboxymethylcellulose (Sigma-Aldrich) and 2.5% FBS. Cultures were incubated at 37 °C with 5% CO_2 for a total post-overlay incubation period of 14 days to permit plaque formation. At the end of the incubation period, monolayers were fixed with 96% methanol (J.T. Baker, Estado de México, Mexico) and stained with 1% crystal violet (Sigma-Aldrich). Plaques were enumerated manually, and viral titers were calculated and expressed as plaque-forming units per milliliter (PFU/mL).

4.4. Preparation of Extracellular Vesicles–Depleted Fetal Bovine Serum (EV-Depleted FBS)

To minimize contamination from serum-derived EVs and ensure the purity of EV isolations, FBS was depleted of EVs prior to use as follows: FBS samples were first clarified by centrifugation at 900× g for 10 min at 4 °C to remove cellular debris and aggregates, followed by filtration through a 0.22 µm pore membrane (Merck, Rahway, NJ, USA). Clarified serum was then ultracentrifuged at 120,000× g for 18 h at 4 °C. The EV-depleted supernatant was carefully recovered, transferred to new sterile conical tubes, and stored at 2 °C until use.

 doi:10.20944/preprints202604.2219.v1

4.5. Monocyte DENV-Infection Assay

Monocytes (Mø; 1.0 × 106 cells) were seeded in 25 cm2 cell culture flasks (Corning) and infected with DENV-2 at a MOI of 1 using non-supplemented RPMI-1640 medium. Viral adsorption was carried out for 2 h at 37 °C with 5% CO2. Cells were harvested and washed with 1× phosphate-buffered saline (PBS), then centrifuged at 550× g for 10 min at rt by duplicate. Cell pellets were resuspended in RPMI-1640 medium supplemented with 5% EVs-depleted FBS and incubated for 72 h.

4.6. Detection of DENV Proteins and Cellular Markers in Monocytes by Flow Cytometry

Monocytes (1.0 × 10^6 cells per condition) were harvested and centrifuged at 550× g (Eppendorf 5415 R centrifuge; Merck, Darmstadt, Germany) for 10 min at 4 °C. Cell pellets were separated from the supernatant, washed with PBS, and fixed with 2% paraformaldehyde (PFA; Sigma-Aldrich) in PBS for 5 min at 4 °C. Following fixation, cells were washed with PBS and incubated with a blocking solution containing 2% bovine serum albumin (BSA; Biowest) in PBS for 30 min at rt to minimize nonspecific antibody binding. Cells were subsequently maintained in 0.5% BSA in PBS at 4 °C.

For direct immunostaining, cells were incubated with fluorophore-conjugated antibodies diluted 1:100 in 0.5% BSA in PBS for 30 min at rt, protected from light. Cells were then washed, centrifuged, resuspended in 0.5% BSA in PBS, and kept at 4 °C until analysis. The following conjugated antibodies were used: phycoerythrin (PE)-conjugated mouse anti-human CD14 IgG1 (clone HCD14; Cat. #325606; BioLegend, San Diego, CA, USA); PE-conjugated mouse anti-human CD11b IgG1 (clone ICRF44; Cat. #301306; BioLegend); and fluorescein isothiocyanate (FITC)-conjugated mouse anti-human CD142 (Cat. #13133-MM05-F; Sino Biological, Wayne, PA, USA).

For indirect immunostaining, cells were incubated with primary antibodies diluted 1:300 in 0.5% BSA in PBS overnight at 4 °C. Cells were subsequently washed with 0.5% BSA in PBS, centrifuged, and incubated with the appropriate fluorophore-conjugated secondary antibody diluted 1:500 in 0.5% BSA in PBS for 2 h at rt, protected from light. After a final washing step, cells were resuspended in 0.5% BSA in PBS. The primary antibodies used were mouse anti-dengue complex monoclonal antibody (clone D3-2H2-9-21; Cat. #MAB8705; Sigma-Aldrich); rabbit anti-dengue virus NS1 protein (Cat. #GTX124280; GeneTex, Irvine, CA, USA); and mouse anti-human CD16 IgG1 (Cat. #555404; BD Pharmingen, BD Biosciences, San Jose, CA, USA). The secondary antibodies employed were Alexa Fluor 555-conjugated donkey anti-mouse IgG (Cat. #A-31570; Thermo Fisher Scientific, Waltham, MA, USA) and Alexa Fluor 488-conjugated donkey anti-rabbit IgG (Cat. #711-546-152; Jackson ImmunoResearch, West Grove, PA, USA).

For phosphatidylserine (PS) detection using an Annexin V binding assay, cells were resuspended in 1× Annexin V binding buffer (Cat. #556454; BD Pharmingen) and incubated with FITC-conjugated Annexin V (Cat. #640906; BioLegend) for 30 min at rt under constant agitation. Following incubation, samples were washed twice, centrifuged, and finally resuspended in Annexin V binding buffer protected from light.

Unstained cells were used as negative controls and the following antibodies were used as isotype controls: PE-conjugated mouse IgG1 antibody (clone MOPC-21; Cat. #400112; BioLegend); FITC-conjugated mouse IgG1 antibody (clone MOPC-21; Cat. #400107; BioLegend); Mouse IgG1 antibody (clone P3.6.2.8.1; Cat. # 14-4714-82; eBioscience, San Diego, CA, USA); and Rabbit polyclonal antibody (clone Poly29108; Cat # 910801; BioLegend). Flow cytometry data acquisition was performed using FACSCalibur (BD Biosciences) and Attune (Applied Biosystems, Thermo Fisher Scientific) flow cytometers (BD Biosciences). Data were collected using CellQuest software and analyzed with FlowJo software version 10.

4.7. Detection of DENV E Protein and Tissue Factor in Monocytes by Immunofluorescence

Monocytes (2.5 × 10^5 cells per condition; DENV-infected and non-infected controls) were seeded onto 8-well chamber slides (Lab-Tek II; Thermo Fisher Scientific). Cells were fixed with 2% PFA for 5

 doi:10.20944/preprints202604.2219.v1

min at 4 °C, followed by washing with 2% BSA in PBS. To reduce nonspecific antibody binding, samples were blocked with 2% BSA in PBS for 30 min at rt and washed with 0.5% BSA in PBS.

For detection of the DENV envelope (E) protein, cells were incubated with a mouse anti-dengue complex monoclonal antibody diluted 1:300 in 0.5% BSA in PBS and maintained overnight at 4 °C under constant agitation. After washing, cells were incubated with an Alexa Fluor 555–conjugated donkey anti-mouse IgG secondary antibody diluted 1:500 for 2 h at rt with constant agitation, protected from light, and then washed with 0.5% BSA in PBS. The mouse IgG1 antibody clone P3.6.2.8.1 was used as isotype control.

For Tissue Factor (TF/CD142) detection, cells were incubated with a FITC-conjugated mouse anti-human CD142 antibody diluted 1:100 in 0.5% BSA in PBS for 2 h at rt in the dark, followed by washing with 0.5% BSA in PBS. The FITC-conjugated mouse IgG1 antibody clone MOPC-21 was used as isotype control.

Finally, slides were mounted using a DAPI-containing mounting medium (AAT Bioquest, Sunnyvale, CA, USA). Immunofluorescence images were acquired using an Olympus IX71 inverted microscope equipped with an Olympus DP72 digital camera (Olympus Corp., Miami, FL, USA), and image analysis was performed with ImageJ software version 1.50i (NIH, Bethesda, MA, USA).

4.8. Ruthenium Red Staining for Evaluation of Monocyte Surface Membranes by Transmission Electron Microscopy (TEM)

Non-infected (Control Mø) and DENV-2-infected monocytes (DENV-2 Mø) were comparatively analyzed by transmission electron microscopy (TEM) using ruthenium red staining to visualize surface carbohydrates at cell membrane. Ruthenium red is a polycationic dye with high affinity for negatively charged carbohydrates and was used following the protocol described by Martinez-Palomo & Brailovski (1968) [52].

Cell samples were fixed and stained with a solution containing 2.5% glutaraldehyde (EMS, Hatfield, PA, USA) and 50 mg/mL ruthenium red (Sigma-Aldrich) in sodium cacodylate buffer (Sigma-Aldrich) for 1 h at rt. After fixation, samples were washed three times with sodium cacodylate buffer and post-fixed with 4% osmium tetroxide (Alfa Aesar, Thermo Fisher Scientific) supplemented with 50 mg/mL ruthenium red for 2 h at rt.

Following post-fixation, samples were washed three times and subjected to dehydration through a graded ethanol (J.T. Baker) series (50%, 60%, 70%, 80%, 90%, 96%, and 100%), with each step performed for 5 min; the absolute ethanol step was repeated three times. Samples were then pre-embedded in a 1:1 mixture of propylene oxide and epoxy resin (Sigma-Aldrich/EMS) for 18 h at rt. After evaporation of propylene oxide, samples were embedded in pure epoxy resin and polymerized at 60 °C for 48 h.

Ultrathin sections (40–50 nm) were obtained using an ultramicrotome and mounted onto formvar-coated copper grids (EMS). Sections were contrasted with uranyl acetate (Merck, Darmstadt, Germany) for 30 min and lead citrate (EMS) for 10 min at rt. Ultrastructural observations were performed using a JEOL JEM-1010 transmission electron microscope equipped with a CCD300-RC digital camera (DAGE-MTI; Michigan City, IN, USA). Image analysis was conducted using ImageJ software.

4.9. Isolation of Monocyte-Derived MPs by Differential Ultracentrifugation

Monocyte culture supernatants were collected into sterile conical tubes (Corning) and subjected to sequential centrifugation steps to isolate monocyte-derived MPs. Initially, samples were centrifuged at 900× g for 10 min at 4 °C to remove intact cells, after which the supernatants were carefully transferred to new tubes and cellular pellets were discarded. The clarified supernatants were then centrifuged at 2,000× g for 10 min at 4 °C to eliminate residual cell debris. Subsequently, supernatants were transferred to sterile ultracentrifuge tubes (25 × 89 mm; Beckman Coulter, Inc.) and centrifuged at 16,500× g for 35 min at 4 °C [53]. Following centrifugation, supernatants were discarded and the resulting MPs pellets were gently resuspended in 1.0 mL of PBS at 4 °C. The MPs

 doi:10.20944/preprints202604.2219.v1

suspensions were collected into sterile microcentrifuge tubes and used immediately for downstream analyses or stored at −72 °C until further use.

4.10. Characterization of Monocyte-Derived MPs by Nanoparticle Tracking Analysis (NTA)

The NTA was conducted using a NanoSight NS300 system (Malvern Panalytical Products, Mexico City, Mexico) to determine the size distribution and concentration of nanoparticles in monocyte-derived EV isolates. Instrument settings for data acquisition were standardized as follows: camera level set to 14, detection threshold of 2.0, and operating temperature maintained at 20 °C. Suspensions of MPs were diluted 1:50 in PBS and a total sample volume of 1.0 mL was loaded for analysis. Each sample was recorded for 90 seconds (s), and measurements were performed in triplicate to ensure analytical consistency. Polystyrene microspheres with a nominal diameter of 100 nm (Cat. #NTA4088; Malvern Panalytical Products), diluted 1:500, were analyzed under identical conditions and used as calibration controls.

4.11. Morphological Characterization of Monocyte-Derived MPs by TEM

Monocyte-derived MPs preparations were fixed using a solution (1:1) containing 2.5% glutaraldehyde and 4% PFA for 2 h at rt. Fixed samples were subsequently post-fixed with 2% osmium tetroxide for 90 min at rt, followed by three washes with PBS. Dehydration was carried out through a graded ethanol series consisting of 30%, 50%, 70%, 80%, 90%, 96%, and absolute ethanol. Dehydrated samples were transitioned through propylene oxide and incubated in a propylene oxide/epoxy resin mixture (1:1) for 18 h at rt, after which they were embedded in pure epoxy resin and polymerized at 60 °C for 48 h. Ultrathin sections were obtained, mounted on grids, contrasted with uranyl acetate for 30 min and lead citrate for 10 min at rt, and examined under a JEM1010 transmission electron microscope equipped with a CCD300-RC digital camera. Image analyses were conducted using ImageJ software.

4.12. Detection of CD14, Tissue Factor (TF, CD142), Phosphatidylserine (PS), and Viral Proteins (E and NS1) in Monocyte-Derived MPs by Flow Cytometry

Monocyte-derived MPs were fixed with 2% PFA for 10 min at 4 °C, centrifuged at 16,500× g for 35 min at 4 °C, and blocked with 2% BSA in PBS for 30 min at rt to minimize nonspecific binding. After blocking, samples were centrifuged and maintained in 0.5% BSA in PBS at 4 °C.

For CD14 and TF detection, MPs were incubated with a PE-conjugated mouse anti-human CD14 antibody or FITC-conjugated mouse anti-human CD142, both diluted 1:100 in 0.5% BSA in PBS. Samples were washed twice with the same buffer and centrifuged. The MPs pellets were then resuspended in 0.5% BSA in PBS. The PE-conjugated mouse IgG1 antibody (clone MOPC-21) and FITC-conjugated mouse IgG1 antibody (clone MOPC-21) were used as isotype controls.

For PS detection, MPs were resuspended in 1× Annexin V binding buffer and incubated with FITC-conjugated Annexin V for 30 min at rt under constant agitation. Following incubation, samples were washed twice with Annexin V binding buffer, centrifuged, and finally resuspended in Annexin V binding buffer, protected from light. Unlabeled MPs were used as negative control.

For viral E and NS1 proteins, MPs were incubated with mouse anti-dengue complex monoclonal antibody or rabbit anti-dengue virus NS1 protein, both diluted at 1:300 in 0.5% BSA in PBS overnight at 4 °C. MPs were subsequently washed with 0.5% BSA in PBS, centrifuged and incubated with Alexa Fluor 555-conjugated donkey anti-mouse IgG or Alexa Fluor 488-conjugated donkey anti-rabbit IgG, both diluted 1:500 in 0.5% BSA in PBS for 2 h at rt, protected from light. MPs were resuspended in 0.5% BSA in PBS. The mouse IgG1 antibody (clone P3.6.2.8.1) and rabbit polyclonal antibody (clone Poly29108) were used as isotype controls.

Microbead NIST Traceable Particle Size Standard of 1.00 μm (Cat. # 608570; Polysciences, Inc., Warrington, PA, USA) and latex beads of 0.1 μm (Cat. # LB1-1ML; Merck) were used as calibrators and controls. Flow cytometric acquisition was performed using an Attune flow cytometer.

 doi:10.20944/preprints202604.2219.v1

4.13. Virion Inactivation in MPs Derived from DENV-Infected Monocytes

To eliminate free viral particles or genomic RNA potentially present in DENV-2-infected Mø MP isolates (DENV-2 Mø MPs), sterile microcentrifuge tubes containing the samples were subjected to ultraviolet (UV) irradiation. Samples were exposed to UV radiation at an energy of 1200 µJ (×100) for three consecutive cycles using a Stratalinker 1800 system (Stratagene, San Diego, CA, USA). Following UV treatment, samples were washed twice with PBS and re-pelleted by centrifugation at 16,500× g for 35 min at 4 °C prior to downstream assays or temporarily stored at 4 °C until use. These isolates were identified as DENV-2 Mø MPs-UV.

4.14. Assessment of Infectious DENV Virions Associated with MP Isolates by Plaque Assay

To determine whether infectious dengue virus (DENV) virions were associated with MP isolates, infectivity was evaluated by plaque assay using Vero cells. Following isolation, the samples of MPs were subjected to UV irradiation as described in section 4.13. After UV treatment, pellets were washed twice with PBS and re-pelleted by centrifugation at 16,500× g for 35 min at 4 °C to remove unbound viral material. Pellets were resuspended in non-supplemented DMEM. Plaque assays were performed as described in section 4.13. Viral stock was included as positive control, while MPs isolated from non-infected monocytes (Control Mø MPs) were used as a negative control.

4.15. Thrombin Generation Assay Mediated by Monocyte Microparticles

The assay was adapted from previous studies by Nieuwland et al. (2000) and Berckmans et al. (2001) [54,55]. Briefly, thrombin generation was initiated by adding 60 µL of prewarned normal plasma (37 °C) to a reaction mixture (Mix A) containing 5 µL of Buffer A (50 mmol/L Tris-HCl [Sigma-Aldrich], 100 mmol/L NaCl [J.T.Baker], and 0.05% BSA [pH 7.35]), 10 µL of monocyte MP isolates (highly concentrated samples), and 15 µL of CaCl2 (Sigma-Aldrich), achieving a final concentration of 17 mmol/L in a total volume of 90 µL. Samples were incubated for 24 h at 37 °C.

After the incubation, 20 µL aliquots from Mix A were added to 55 µL of prewarmed Buffer B (50 mmol/L Tris-HCl, 100 mmol/L NaCl, 29 mmol/L EDTA [J.T.Baker], and 0.05% BSA (pH 7.9)] containing 2 mmol/L of the chromogenic substrate S-2238 (Chromogenix S-2238; Cat # S820324; DiaPharma, OH, USA) resulting in a final volume of 75 µL.

The reaction mixture was incubated at 37 °C, and substrate cleavage was stopped at 5 and 20 min by adding 90 µL of 1 mol/L citric acid (J.T.Baker). The generation of p-nitroaniline was quantified by measuring absorbance at 405 nm.

4.16. Protein Quantification in Isolates of Monocyte-Derived MPs by Micro BCA Protein Assay

Protein concentration was determined using the Micro BCA Protein Assay Kit (Thermo Fisher Scientific), according to the manufacturer's instructions. Briefly, a calibration curve was generated using twofold serial dilutions prepared from a 2 mg/mL BSA standard. Volumes of 150 µL of blanks, standards, and samples were loaded in duplicate into flat-bottom 96-well microplates (Corning), followed by the addition of 150 µL of the working reagent mixture. Plates were incubated at 37 °C for 2 h, and absorbance was measured at 562 nm.

4.17. Stimulation of Naïve Endothelial Vascular Cells (EVC) with Monocyte-Derived MPs

Naïve EVC (1.0×10^6 cells per condition) seeded in 25 cm2 cell culture flasks (Corning) were exposed to monocyte-derived MPs (Control Mø MPs, DENV-2 Mø MPs, and DENV-2 Mø MPs-UV) normalized to a total protein content of 1.0 mg/mL. Stimulation was performed in serum-free MCDB-131 medium and maintained for 2 h at 37 °C with a 5% CO_2 to allow initial interaction. Subsequently, culture medium supplemented with 5% EVs-depleted FBS was added, and cells were further incubated for 72 h under the same conditions. At the end of the incubation period, endothelial cells were harvested by trypsinization (TypLE Express; Cat. #12604-013; Gibco, Life Technologies

 doi:10.20944/preprints202604.2219.v1

Corporation, NY, USA) and collected by centrifugation at 550× g for 10 min at 4 °C for downstream analyses.

4.18. Detection of Viral Proteins and Cellular Markers in EVC by Flow Cytometry

Monocyte-derived MPs-stimulated EVC were fixed with 2% PFA in PBS for 5 min at 4 °C. Following fixation, cells were washed with PBS, incubated with 2% BSA in PBS for 30 min at rt to minimize nonspecific antibody binding, and maintained in 0.5% BSA in PBS at 4 °C. Cells were processed for immunostaining as described in section 4.6.

For direct immunostaining, the following fluorophore-conjugated antibodies were used: FITC-conjugated mouse anti-human CD142; FITC-conjugated mouse anti-human ICAM-1 (CD54; Cat. #35-0549-T025; Tonbo Biosciences, San Diego, CA, USA); and PE-conjugated mouse anti-human VCAM-1 (Cat. #sc-13160; Santa Cruz Biotechnology, Dallas, TX, USA). The FITC-conjugated mouse IgG1 antibody (clone MOPC-21) and PE-conjugated mouse IgG1 antibody (clone MOPC-21) and were used as isotype controls.

For indirect immunostaining, mouse anti-human protease-activated receptor-1 (PAR-1) antibody (Cat. #SC-13503; Santa Cruz Biotechnology), mouse anti-dengue complex monoclonal antibody, and rabbit anti-dengue virus NS1 protein, all diluted at 1:300, were used as primary antibodies. Alexa Fluor 555-conjugated donkey anti-mouse IgG or Alexa Fluor 488-conjugated donkey anti-rabbit IgG, both diluted 1:500, were used as secondary antibodies. The mouse IgG1 antibody (clone P3.6.2.8.1) and rabbit polyclonal antibody (clone Poly29108) were used as isotype controls. Flow cytometric analysis was performed using an Attune flow cytometer.

4.19. Assessment of EVC Permeability by Transwell Assay

Confluent EVC monolayers (3.5 × 105 cells per condition) were grown on the upper inserts of sterile polycarbonate, tissue culture–treated transwell plates (Cat. #3401, Corning). Both upper inserts and lower chambers contained MCDB-131 medium supplemented with EV-depleted FBS. Confluent monolayers were exposed to monocyte-derived MPs normalized to a final concentration of 1 mg/mL of total protein in non-supplemented MCDB-131 medium and incubated for 2 h at 37 °C with 5% CO_2. Then, medium supplemented with 5% EV-depleted FBS was added, and transwell plates were incubated for 48 h under the same conditions.

To evaluate endothelial permeability, FITC–labeled dextran (40 kDa; Cat. # 60842-46-8, Sigma-Aldrich) diluted 1:60 in MCDB-131 medium supplemented with 5% EV-depleted FBS was added to the upper chamber and incubated for 1 h at 37 °C. After incubation, aliquots of medium from the lower chamber were collected, diluted 1:50 in PBS, and transferred to black 96-well plates (Corning) for fluorescence measurement. Inserts without cells containing FITC–dextran was included as no-cell controls (NCC) and defined as the 100% permeability reference.

Fluorescence intensity corresponding to FITC–dextran that crossed the endothelial monolayer was measured at excitation/emission wavelengths of 492/520 nm. Endothelial permeability was expressed as a percentage and calculated using the formula: p% = (Abs sample / Abs NCC) × 100, where Abs sample corresponds to the absorbance values of experimental or control samples and Abs NCC represents the absorbances values of the NCC.

4.20. Statistical Analysis

Data was obtained from three to five independent experiments. Flow cytometry data was analyzed using FlowJo software version 10 (BD Biosciences). Quantitative results are presented as the mean ± standard deviation (SD) and statistical analyses were performed using GraphPad Prism software version 10.6.1 (GraphPad Software Inc., San Diego, CA, USA).

For comparisons between two independent groups, an unpaired Student's *t*-test with Welch's correction was applied. Multiple comparisons across different experimental conditions and time points (Thrombin generation assays) were analyzed using two-way analysis of variance (ANOVA),

 doi:10.20944/preprints202604.2219.v1

followed by Tukey's *post hoc* test with Holm–Šidák correction for multiple testing. For monocyte-derived MPs stimulation assays, including permeability assays, differences among groups were evaluated using one-way ANOVA followed by Dunnett's T3 *post hoc* test. Statistical significance was defined as * $p < 0.05$, ** $p < 0.01$, and *** $p < 0.0001$.

Supplementary Materials: This article does not include supplementary materials.

Author Contributions: Conceptualization, J.G.-P and B.H.R.-O.; methodology, J.G.-P., P.P.M.-R., E.Q.-G., C.C.-G., M.L., L.P.-N., L.T.A.-M., L.F.J.-G., and B.H.R.-O.; validation, C.C.-G., M.L., L.P.-N.; formal analysis, J.G.-P., P.P.M.-R., E.Q.-G., L.T.A.-M., and B.H.R.-O.; investigation, J.G.-P. and B.H.R.O.; resources, C.C.-G., L.F.J.-G, and B.H.R.-O; writing—original draft preparation, J.G.-P., P.P.M.-R., and B.H.R.-O.; writing—review and editing, J.G.-P., M.L., L.P.-N., and B.H.R.-O; supervision, B.H.R.-O.; project administration, P.P.M.-R.; funding acquisition, B.H.R.-O. All authors have read and agreed to the published version of the manuscript.

Funding: This research was funded by the Programa de Apoyo a Proyectos de Investigación e Innovación Tecnológica (PAPIIT), administered by the Dirección General de Asuntos del Personal Académico (DGAPA) at the Universidad Nacional Autónoma de México (UNAM), under grant number IN224923.

Institutional Review Board Statement: Not applicable.

Informed Consent Statement: Not applicable.

Data Availability Statement: The original contributions presented in this study are included in the article, further inquiries can be directed to the corresponding author.

Acknowledgments: Janet García-Pillado is a doctoral fellow in the Programa de Maestría y Doctorado en Ciencias Bioquímicas at the Universidad Nacional Autónoma de México (UNAM) and received a scholarship from the Secretaría de Ciencia, Humanidades, Tecnología e Innovación (Secihti). The authors gratefully acknowledge the support provided by PAPIIT-UNAM, the LabNalCit-UNAM (Secihti) for the technical support in the acquisition of flow cytometry samples, and Miguel Tapia Rodríguez from Unidad de Microscopía at Instituto de Investigaciones Biomédicas UNAM, for his support in the use of microscopes.

Conflicts of Interest: The authors declare no conflicts of interest. The funders had no role in the design of the study; in the collection, analyses, or interpretation of data; in the writing of the manuscript; or in the decision to publish the results.

Abbreviations

The following abbreviations are used in this manuscript:

CD	Cluster of differentiation
DENV	Dengue virus
DENV E	Dengue virus envelope protein
DENV NS1	Dengue virus nonstructural protein 1
DENV-2 Mø MPs	Microparticles derived from dengue virus-infected monocytes
DF	Dengue fever
EVC	Endothelial vascular cells
EVs	Extracellular vesicles
ICAM-1	Intercellular adhesion molecule 1
IL	Interleukin
MPs	Microparticles
Mø	Monocytes
mRNA	Messenger ribonucleic acid
NTA	Nanoparticle tracking analysis
TEM	Transmission electron microscopy
TF	Tissue Factor
TNF-α	Tumor necrosis factor alpha
SD	Severe dengue
PAR-1	Protease-activated receptor 1

 doi:10.20944/preprints202604.2219.v1

PS	Phosphatidylserine
VCAM-1	Vascular cell adhesion molecule 1

References

1. World Health Organization (WHO). Dengue. Available online: https://www.who.int/news-room/fact-sheets/detail/dengue-and-severe-dengue (accessed on 28 January 2026).
2. Yang, Z.S.; Baua, A.D.; Hemdan, M.S.; Assavalapsakul, W.; Wang, W.H.; Lin, C.Y.; Chao, D.Y.; Chen, Y.H.; Wang, S.F. Dengue virus infection: A systematic review of pathogenesis, diagnosis and management. *J. Infect. Public. Health.* **2025**, *18*, 102982. doi: 10.1016/j.jiph.2025.102982.
3. Kothari, D.; Patel, N.; Bishoyi, A.K. Dengue: epidemiology, diagnosis methods, treatment options, and prevention strategies. *Arch. Virol.* **2025**, *170*, 48. doi: 10.1007/s00705-025-06235-3.
4. World Health Organization (WHO); Special Programme for Research and Training in Tropical Diseases (TDR). *Dengue: Guidelines for Diagnosis, Treatment, Prevention and Control, New Edition*; WHO Press: Geneva, Switzerland, 2009; pp. 10-13.
5. Aguilar-Briseño, J.A.; Upasani, V.; Ellen, B.M.T.; Moser, J.; Pauzuolis, M.; Ruiz-Silva, M.; Heng, S.; Laurent, D.; Choeung, R.; Dussart, P.; et al. TLR2 on blood monocytes senses dengue virus infection and its expression correlates with disease pathogenesis. *Nat. Commun.* **2020**, *11*, 3177. doi: 10.1038/s41467-020-16849-7.
6. Castillo, J.A.; Naranjo, J.S.; Rojas, M.; Castaño, D.; Velilla, P.A. Role of Monocytes in the Pathogenesis of Dengue. *Arch. Immunol. Ther. Exp. (Warsz).* **2019**, *67*, 27-40. doi: 10.1007/s00005-018-0525-7.
7. Lertjuthaporn, S.; Keawvichit, R.; Polsrila, K.; Sukapirom, K.; Chuansumrit, A.; Chokephaibulkit, K.; Ansari, A.A.; Khowawisetsut, L.; Pattanapanyasat, K. Kinetic Changes of Peripheral Blood Monocyte Subsets and Expression of Co-Stimulatory Molecules during Acute Dengue Virus Infection. *Pathogens.* **2021**, *10*, 1458. doi: 10.3390/pathogens10111458.
8. Dunagan, M.M.; Fox, J.M. Splenic macrophages escalate dengue disease. *Nat. Microbiol.* **2023**, *8*, 1378-1379. doi: 10.1038/s41564-023-01437-4.
9. Flipse, J.; Torres, S.; Diosa-Toro, M.; van der Ende-Metselaar, H.; Herrera-Rodriguez, J.; Urcuqui-Inchima, S.; Huckriede, A.; Rodenhuis-Zybert, I.A.; Smit, J.M. Dengue tropism for macrophages and dendritic cells: the host cell effect. *J. Gen. Virol.* **2016**, *97*, 1531-1536. doi: 10.1099/jgv.0.000474.
10. Losada, P.X.; DeLaura, I.; Narváez, C.F. Dengue Virus and Platelets: From the Biology to the Clinic. *Viral. Immunol.* **2022**, *35*, 349-358. doi: 10.1089/vim.2021.0135.
11. Quirino-Teixeira, A.C.; Andrade, F.B.; Pinheiro, M.B.M.; Rozini, S.V.; Hottz, E.D. Platelets in dengue infection: more than a numbers game. *Platelets.* **2022**, *33*, 176-183. doi: 10.1080/09537104.2021.1921722.
12. Vervaeke, P.; Vermeire, K.; Liekens, S. Endothelial dysfunction in dengue virus pathology. *Rev. Med. Virol.* **2015**, *25*, 50-67. doi: 10.1002/rmv.1818.
13. Malavige, G.N.; Ogg, G.S. Pathogenesis of vascular leak in dengue virus infection. *Immunology.* **2017**, *151*, 261-269. doi: 10.1111/imm.12748.
14. Naranjo-Gómez, J.S.; Castillo, J.A.; Rojas, M.; Restrepo, B.N.; Diaz, F.J.; Velilla, P.A.; Castaño, D. Different phenotypes of non-classical monocytes associated with systemic inflammation, endothelial alteration, and hepatic compromise in patients with dengue. *Immunology.* **2019**, *156*, 147-163. doi: 10.1111/imm.13011.
15. Wong, K.L.; Chen, W.; Balakrishnan, T.; Toh, Y.X.; Fink, K.; Wong, S.C. Susceptibility and response of human blood monocyte subsets to primary dengue virus infection. *PLoS One* **2012**, *7*, e36435. doi: 10.1371/journal.pone.0036435.
16. Silva, T.; Gomes, L.; Jeewandara, C.; Ogg, G.S.; Malavige, G.N. Dengue NS1 induces phospholipase A2 enzyme activity, prostaglandins, and inflammatory cytokines in monocytes. *Antiviral. Res.* **2022**, *202*, 105312. doi: 10.1016/j.antiviral.2022.105312.
17. Beltrami, S.; Ferraresi, M.; Cianci, G.; Narducci, M.; Rizzo, R.; Baroni, M.; Bortolotti, D. Flavivirus Nonstructural Protein 1-Driven Coagulation via Tissue Factor-Bearing Microvesicles: A Pilot Study. *ACS. Omega.* **2025**, *10*, 56645-56655. doi: 10.1021/acsomega.5c09129.

 doi:10.20944/preprints202604.2219.v1

18. de Azeredo, E.L.; Kubelka, C.F.; Alburquerque, L.M.; Barbosa, L.S.; Damasco, P.V.; Avila, C.A.; Motta-Castro, A.R.; da Cunha, R.V.; Monteiro, R.Q. Tissue factor expression on monocytes from patients with severe dengue fever. *Blood. Cells. Mol. Dis.* **2010**, *45*, 334-5. doi: 10.1016/j.bcmd.2010.08.004.
19. Martins, S.T.; Kuczera, D.; Lötvall, J.; Bordignon, J.; Alves, L.R. Characterization of Dendritic Cell-Derived Extracellular Vesicles During Dengue Virus Infection. *Front. Microbiol.* **2018**, *9*, 1792. doi: 10.3389/fmicb.2018.01792.
20. Welsh, J.A.; Goberdhan, D.C.I.; O'Driscoll, L.; Buzas, E.I.; Blenkiron, C.; Bussolati, B.; Cai, H.; Di Vizio, D.; Driedonks, T.A.P.; Erdbrügger, U.; et al. Minimal information for studies of extracellular vesicles (MISEV2023): From basic to advanced approaches. *J. Extracell. Vesicles.* **2024**, *13*, e12404. doi: 10.1002/jev2.12404.
21. Russell, A.E.; Sneider, A.; Witwer, K.W.; Bergese, P.; Bhattacharyya, S.N.; Cocks, A.; Cocucci, E.; Erdbrügger, U.; Falcon-Perez, J.M.; Freeman, D.W.; et al. Biological membranes in EV biogenesis, stability, uptake, and cargo transfer: an ISEV position paper arising from the ISEV membranes and EVs workshop. *J. Extracell. Vesicles.* **2019**, *8*, 1684862. doi: 10.1080/20013078.2019.1684862.
22. Théry, C.; Witwer, K.W.; Aikawa, E.; Alcaraz, M.J.; Anderson, J.D.; Andriantsitohaina, R.; Antoniou, A.; Arab, T.; Archer, F.; Atkin-Smith, G.K.; et al. Minimal information for studies of extracellular vesicles 2018 (MISEV2018): a position statement of the International Society for Extracellular Vesicles and update of the MISEV2014 guidelines. *J. Extracell. Vesicles.* **2018**, *7*, 1535750. doi: 10.1080/20013078.2018.1535750.
23. Cocucci, E.; Meldolesi, J. Ectosomes and exosomes: shedding the confusion between extracellular vesicles. *Trends. Cell. Biol.* **2015**, *25*, 364-372. doi: 10.1016/j.tcb.2015.01.004.
24. Voukalis, C.; Shantsila, E.; Lip, G.Y.H. Microparticles and cardiovascular diseases. *Ann. Med.* **2019**, *51*, 193-223. doi: 10.1080/07853890.2019.1609076.
25. Lugo-Gavidia, L.M.; Burger, D.; Matthews, V.B.; Nolde, J.M.; Galindo Kiuchi, M.; Carnagarin, R.; Kannenkeril, D.; Chan, J.; Joyson, A.; Herat, L.Y.; et al. Role of Microparticles in Cardiovascular Disease: Implications for Endothelial Dysfunction, Thrombosis, and Inflammation. *Hypertension.* **2021**, 77, 1825-1844. doi: 10.1161/HYPERTENSIONAHA.121.16975.
26. Singh, A.; Bisht, P.; Bhattacharya, S.; Guchhait, P. Role of Platelet Cytokines in Dengue Virus Infection. *Front. Cell. Infect. Microbiol.* **2020**, *10*, 561366. doi: 10.3389/fcimb.2020.561366.
27. Hottz, E.D.; Lopes, J.F.; Freitas, C.; Valls-de-Souza, R.; Oliveira, M.F.; Bozza, M.T.; Da Poian, A.T.; Weyrich, A.S.; Zimmerman, G.A.; Bozza, F.A.; et al. Platelets mediate increased endothelium permeability in dengue through NLRP3-inflammasome activation. *Blood.* **2013**, *122*, 3405-3414. doi: 10.1182/blood-2013-05-504449.
28. Patil, R.; Bajpai, S.; Ghosh, K.; Shetty, S. Microparticles as prognostic biomarkers in dengue virus infection. *Acta. Trop.* **2018**, *181*, 21-24. doi: 10.1016/j.actatropica.2018.01.017.
29. Punyadee, N.; Mairiang, D.; Thiemmeca, S.; Komoltri, C.; Pan-Ngum, W.; Chomanee, N.; Charngkaew, K.; Tangthawornchaikul, N.; Limpitikul, W.; Vasanawathana. S.; et al. Microparticles provide a novel biomarker to predict severe clinical outcomes of dengue virus infection. *J. Virol.* **2015**, *89*, 1587-1607. doi: 10.1128/JVI.02207-14.
30. Martínez-Rojas, P.P.; Monroy-Martínez, V.; Agredano-Moreno, L.T.; Jiménez-García, L.F.; Ruiz-Ordaz, B.H. Zika Virus-Infected Monocyte Exosomes Mediate Cell-to-Cell Viral Transmission. *Cells.* **2024**, *13*, 144. doi: 10.3390/cells13020144.
31. Meerschaert, J.; Furie, M.B. The adhesion molecules used by monocytes for migration across endothelium include CD11a/CD18, CD11b/CD18, and VLA-4 on monocytes and ICAM-1, VCAM-1, and other ligands on endothelium. *J. Immunol.* **1995**, *154*, 4099-112.
32. Osterud, B. Cellular interactions in tissue factor expression by blood monocytes. *Blood. Coagul. Fibrinolysis.* **1995**, *6*, S20-5.
33. Herring, J.M.; McMichael, M.A.; Smith, S.A. Microparticles in health and disease. *J. Vet. Intern. Med.* **2013**, *27*, 1020-1033. doi: 10.1111/jvim.12128.
34. van Niel, G.; D'Angelo, G.; Raposo, G. Shedding light on the cell biology of extracellular vesicles. *Nat. Rev. Mol. Cell Biol.* **2018**, *19*, 213-228. doi: 10.1038/nrm.2017.125.
35. Nour, A.M.; Modis, Y. Endosomal vesicles as vehicles for viral genomes. *Trends. Cell. Biol.* **2014**, *24*, 449-54. doi: 10.1016/j.tcb.2014.03.006.

 doi:10.20944/preprints202604.2219.v1

36. Bargeron Clark, K.; Hsiao, H.M.; Noisakran, S.; Tsai, J.J.; Perng, G.C. Role of microparticles in dengue virus infection and its impact on medical intervention strategies. *Yale. J. Biol. Med.* **2012**, *85*, 3-18.
37. Latanova, A.; Karpov, V.; Starodubova, E. Extracellular Vesicles in Flaviviridae Pathogenesis: Their Roles in Viral Transmission, Immune Evasion, and Inflammation. *Int. J. Mol. Sci.* **2024**, *25*, 2144. doi: 10.3390/ijms25042144.
38. Ishikawa, T.; Narita, K.; Matsuyama, K.; Masuda, M. Dissemination of the Flavivirus Subgenomic Replicon Genome and Viral Proteins by Extracellular Vesicles. *Viruses.* **2024**, *16*, 524. doi: 10.3390/v16040524.
39. Puerta-Guardo, H.; Glasner, D.R.; Espinosa, D.A.; Biering, S.B.; Patana, M.; Ratnasiri, K.; Wang, C.; Beatty, P.R.; Harris, E. Flavivirus NS1 Triggers Tissue-Specific Vascular Endothelial Dysfunction Reflecting Disease *Tropism. Cell. Rep.* **2019**, *26*, 1598-1613.e8. doi: 10.1016/j.celrep.2019.01.036.
40. Shu, B.; Ooi, J.S.G.; Tan, A.W.K.; Ng, T.S.; Dejnirattisai, W.; Mongkolsapaya, J.; Fibriansah, G.; Shi, J.; Kostyuchenko, V.A.; Screaton, G.R.; et al. CryoEM structures of the multimeric secreted NS1, a major factor for dengue hemorrhagic fever. *Nat. Commun.* **2022**, *13*, 6756. doi: 10.1038/s41467-022-34415-1.
41. Safadi, D.E.; Lebeau, G.; Lagrave, A.; Mélade, J.; Grondin, L.; Rosanaly, S.; Begue, F.; Hoareau, M.; Veeren, B.; Roche, M.; et al. Extracellular Vesicles Are Conveyors of the NS1 Toxin during Dengue Virus and Zika Virus Infection. *Viruses.* **2023**, *15*, 364. doi: 10.3390/v15020364.
42. Huerta-Zepeda, A.; Cabello-Gutiérrez, C.; Cime-Castillo, J.; Monroy-Martínez, V.; Manjarrez-Zavala, M.E.; Gutiérrez-Rodríguez, M.; Izaguirre, R.; Ruiz-Ordaz, B.H. Crosstalk between coagulation and inflammation during Dengue virus infection. *Thromb. Haemost.* **2008**, *99*, 936-43. doi: 10.1160/TH07-08-0438.
43. World Health Organization, Ministry of Health of Democratic Republic of Timor-Leste. National Guideline for Clinical Management of Dengue 2022. Timor-Leste: World Health Organization. Available online: https://cdn.who.int/media/docs/default-source/2021-dha-docs/5_national-clinical-guideline-of-dengue-timor-leste_clean_final-12-dec-2022.pdf?sfvrsn=e80bf9cd_1 (accessed on 1 April 2026).
44. Nascimento, E.J.; Hottz, E.D.; Garcia-Bates, T.M.; Bozza, F.; Marques, E.T. Jr.; Barratt-Boyes, S.M. Emerging concepts in dengue pathogenesis: interplay between plasmablasts, platelets, and complement in triggering vasculopathy. *Crit. Rev. Immunol.* **2014**, *34*, 227-40. doi: 10.1615/critrevimmunol.2014010212.
45. Pozo-Aguilar, J.O.; Monroy-Martínez, V.; Díaz, D.; Barrios-Palacios, J.; Ramos, C.; Ulloa-García, A.; García-Pillado, J.; Ruiz-Ordaz BH. Evaluation of host and viral factors associated with severe dengue based on the 2009 WHO classification. *Parasit. Vectors.* **2014**, *7*, 590. doi: 10.1186/s13071-014-0590-7.
46. Rovai, E.S.; Alves, T.; Holzhausen, M. Protease-activated receptor 1 as a potential therapeutic target for COVID-19. *Exp. Biol. Med. (Maywood).* **2021**, *246*, 688-694. doi: 10.1177/1535370220978372.
47. Flaumenhaft, R. Protease-Activated Receptor-1 Signaling: The Big Picture. *Arterioscler. Thromb. Vasc. Biol.* **2017**, *37*, 1809-1811. doi: 10.1161/ATVBAHA.117.310068.
48. Mutiara Koh, S.C.L.; Bachtiar, A.; Hariman, H. The Vascular Endothelium in Patients with Dengue Haemorrhagic Fever. *Open Access Maced. J. Med. Sci.* **2019**, *7*, 2221-2225. doi: 10.3889/oamjms.2019.621.
49. Ghita, L.; Yao, Z.; Xie, Y.; Duran, V.; Cagirici, H.B.; Samir, J.; Osman, I.; Rebellón-Sánchez, D.E.; Agudelo-Rojas, O.L.; Sanz, A.M.; et al. Global and cell type-specific immunological hallmarks of severe dengue progression identified via a systems immunology approach. *Nat. Immunol.* **2023**, *24*, 2150-2163. doi: 10.1038/s41590-023-01654-3.
50. Martínez-Rojas, P.P.; Monroy-Martínez, V.; Ruiz-Ordaz, B.H. Role of extracellular vesicles in the pathogenesis of mosquito-borne flaviviruses that impact public health. *J. Biomed. Sci.* **2025**, *32*, 4. doi: 10.1186/s12929-024-01096-5.
51. Mishra, R.; Lata, S.; Ali, A.; Banerjea, A.C. Dengue haemorrhagic fever: a job done via exosomes? *Emerg. Microbes. Infect.* **2019**, *8*, 1626-1635. doi: 10.1080/22221751.2019.1685913.
52. Martinez-Palomo, A.; Brailovski, C. Surface layer in tumor cells transformed by adeno-12 and SV40 viruses. *Virology.* **1968**, *34*, 379-82. doi: 10.1016/0042-6822(68)90255-9.
53. Lässer, C.; Eldh, M.; Lötvall, J. Isolation and characterization of RNA-containing exosomes. *J. Vis. Exp.* **2012**, *59*, e3037. doi: 10.3791/3037.

 doi:10.20944/preprints202604.2219.v1

54. Nieuwland, R.; Berckmans, R.J.; McGregor, S.; Böing, A.N.; Romijn, F.P.; Westendorp, R.G.; Hack, C.E.; Sturk, A. Cellular origin and procoagulant properties of microparticles in meningococcal sepsis. *Blood.* **2000**, *95*, 930-935. doi: 10.1182/blood.V95.3.930.003k46_930_935.
55. Berckmans, R.J.; Nieuwland, R.; Böing, A.N.; Romijn, F.P.; Hack, C.E.; Sturk, A. Cell-derived microparticles circulate in healthy humans and support low grade thrombin generation. *Thromb. Haemost.* **2001**, *85*, 639-646. doi: 10.1055/s-0037-1615646.